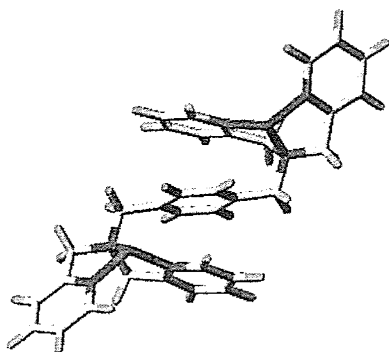

Figure 2. The structure calculated by molecular modeling of compound **2** having the zinc(II)−Dpa structure. Nitrogen atoms, blue; hydrogen atoms, sky blue; zinc atoms, red.

respectively, showed high activity. However, it suggests that the addition of one and two benzene moieties to compound **2** caused a slight decrease in activity. Unexpectedly, an anthracenyl compound having only one [bis(pyridin-2-ylmethyl)-amino]methylene unit with zinc(II) complexation (**13**) exhibited not so high but significant antagonistic activity. It may be reasonable that the anthracenyl compound **15**, which has two sets of this unit at the 1,8-positions, did not show high antagonistic activity, since it is thought to be important that these units are located 180° from each other. In addition, terphenyl compounds **16** and **17** did not show any significant activity until 1 μM, suggesting that it might be unsuitable that two sets of this unit be located far apart from each other.

Next, to investigate whether the location of the nitrogen atom in the pyridine ring of the [bis(pyridin-2-ylmethyl)amino]-methylene unit is critical for expression of CXCR4-antagonistic activity, compounds **18** and **19**, which contained the [bis(pyridin-3-ylmethyl)amino]methylene and [bis(pyridin-4-ylmethyl)amino]methylene units, respectively, with zinc(II) complexation, were synthesized. Neither compound **18** nor **19** showed any significant activity, although antagonistic activity was estimated to 10 μM. This result suggested that the location of the nitrogen atom in the pyridine ring is important either for formation of active conformation or for stable complexation with zinc(II).

Molecular modeling simulation analysis showed that the bis-(3,3′-dipicolylamine) and bis(4,4′-dipicolylamine)-*p*-xylene Zn complexes **18** and **19** did not converge as well as bis(Dpa)−Zn complex **2** did (Figure 2). Values of the coordinate bond lengths between zinc and nitrogen atoms (of the pyridine rings/of the tertiary amine) in the bis(Dpa)−Zn complex **2** are 1.93−1.95 Å, according to molecular modeling calculations. Complex **2** forms a stable conformation, having $\pi-\pi$ stacking among three aromatic rings, as shown in Figure 2. However, values of bond lengths between zinc and nitrogen atoms of the pyridine rings in the complexes **18** and **19** would be ca. 2.9 and ca. 4.2 Å, respectively, which are relatively long. In addition, the proton atoms at the positions 2 and 2′ in the pyridine rings might interfere with the zinc atom to prevent the molecules from forming a stable coordinate conformation.

Furthermore, to verify the indispensability of zinc(II) complexation, zinc-free analogues of **2**, **5**, **7**,and **14**, compounds **20**−**23**, respectively, were assessed for CXCR4-antagonistic activity. Since these zinc-free compounds did not show any significant activity until 10 μM, zinc(II) atoms or conformation constrained by zinc(II) complexation might be indispensable for binding to CXCR4. As a matter of course, zinc-free analogues of **18** and **19**, compounds **24** and **25**, respectively, did not show any significant activity.

Table 4. CXCR4-Binding Activity of Compounds **2**, **5**, **7**, and **12**

compd	IC_{50} (μM)[a]	compd	IC_{50} (μM)[a]
2	0.047	**8** (T140)	0.00093
5	0.18	**9** (FC131)	0.0030
7	0.22	**10** (KRH-1636)	0.034
12	0.42		

[a] IC_{50} values are based on the inhibition of [^{125}I]CXCL12 binding to CXCR4 transfectants of CHO cells. All data are the mean values for at least two independent experiments.

Next, we investigated CXCR4-binding activity of the novel compounds that possess strong CXCR4-antagonistic activity (Table 4). Compounds **2**, **5**, **7**, and **12** showed potent binding activity. Especially, the potency of compound **2** is comparable to that of KRH-1636.

The best and simple compound among the present compounds (**2**) was evaluated for anti-HIV activity. Compound **2** showed significant inhibitory activity against X4-HIV-1-induced cytopathogenicity in MT-4 cells (EC_{50} = 7.1 μM), although anti-HIV activity in cells is lower than CXCR4-antagonistic or -binding activity as usual.[23] Furthermore, the present compounds identified as CXCR4 antagonists showed no significant inhibition (<25%) at 10 μM against Ca^{2+} mobilization induced by MIP-1α stimulation through CCR5 and at 30 μM against Ca^{2+} mobilization induced by sphingosine 1-phosphate stimulation through EDG3 (GPCR).

The present compounds, such as **2**, **5**, **7**, and **12**, have been prepared as binuclear zinc complexes for the use in several assays. The extracellular concentration of zinc is normally ~100 μg/100 mL (approximately 15 μM): 30% of the total zinc is tightly bound to the metal-binding proteins. The remaining amount (70%) is loosely bound to proteins and easily released from the corresponding proteins.[31] Thus, the extracellular concentration of zinc is sufficiently high for the compounds to be active in vivo. Furthermore, the dipicolylamine (Dpa) unit forms a stable complex with zinc ion (log $K = 7.57$), indicating that the compounds can maintain an active state as the zinc complex in vivo. The affinity of the Dpa unit for Ca^{2+} and Mg^{2+} ions, which are biologically essential, is considerably low (log $K < 3$). Thus, it is thought that these ions might not affect the zinc complexes.

Conclusion

The current study presents a new class of nonpeptide CXCR4 antagonists with low molecular weight that have a novel scaffold: a dipicolylamine−zinc(II) complex structure. These compounds showed selective and strong CXCR4-antagonistic activity. These compounds also have basic and aromatic moieties in common with several reported CXCR4 antagonists, e.g., T140, FC131, AMD3100 and KRH-1636, suggesting that these moieties are critical for interaction with CXCR4. The present results provide useful insights for the future design of new CXCR4 antagonists in association with information from other CXCR4 antagonists for development of therapeutic strategies for CXCR4-relevant diseases. Furthermore, anthracene derivatives having two sets of zinc(II)−dipicolylamine, such as compound **14**, might be used as chemical probes to study the biology of CXCR4, as these compounds are used to sense phosphorylated peptide surfaces.

Acknowledgment. This work was supported in part by a 21st Century COE Program "Knowledge Information Infrastructure for Genome Science", a Grant-in-Aid for Scientific Research from the Ministry of Education, Culture, Sports, Science and Technology, Japan, and the Japan Health Science Foundation.

Supporting Information Available: Additional experimental procedures of novel synthetic compounds. This material is available free of charge via the Internet at http://pubs.acs.org.

References

(1) Nagasawa, T.; Kikutani, H.; Kishimoto, T. Molecular cloning and structure of a pre-B-cell growth-stimulating factor. *Proc. Natl. Acad. Sci. U.S.A.* **1994**, *91*, 2305–2309.
(2) Bleul, C. C.; Farzan, M.; Choe, H.; Parolin, C.; Clark-Lewis, I.; Sodroski, J.; Springer, T. A. The lymphocyte chemoattractant SDF-1 is a ligand for LESTR/fusin and blocks HIV-1 entry. *Nature* **1996**, *382*, 829–833.
(3) Oberlin, E.; Amara, A.; Bachelerie, F.; Bessia, C.; Virelizier, J.-L.; Arenzana-Seisdedos, F.; Schwartz, O.; Heard, J.-M.; Clark-Lewis, I.; Legler, D. F.; Loetscher, M.; Baggiolini, M.; Moser, B. The CXC chemokine SDF-1 is the ligand for LESTR/fusin and prevents infection by T-cell-line-adapted HIV-1. *Nature* **1996**, *382*, 833–835.
(4) Tashiro, K.; Tada, H.; Heilker, R.; Shirozu, M.; Nakano, T.; Honjo, T. Signal sequence trap: A cloning strategy for secreted proteins and type I membrane proteins. *Science* **1993**, *261*, 600–603.
(5) Feng, Y.; Broder, C. C.; Kennedy, P. E.; Berger, E. A. HIV-1 entry co-factor: Functional cDNA cloning of a seven-transmembrane, G protein-coupled receptor. *Science* **1996**, *272*, 872–877.
(6) Koshiba, T.; Hosotani, R.; Miyamoto, Y.; Ida, J.; Tsuji, S.; Nakajima, S.; Kawaguchi, M.; Kobayashi, H.; Doi, R.; Hori, T.; Fujii, N.; Imamura, M. Expression of stromal cell-derived factor 1 and CXCR4 ligand receptor system in pancreatic cancer: A possible role for tumor progression. *Clin. Cancer. Res.* **2000**, *6*, 3530–3535.
(7) Müller, A.; Homey, B.; Soto, H.; Ge, N.; Catron, D.; Buchanan, M. E.; McClanahan, T.; Murphy, E.; Yuan, W.; Wagner, S. N.; Barrera, J. L.; Mohar, A.; Verastegui, E.; Zlotnik, A. Involvement of chemokine receptors in breast cancer metastasis. *Nature* **2001**, *410*, 50–56.
(8) Tamamura, H.; Hori, A.; Kanzaki, N.; Hiramatsu, K.; Mizumoto, M.; Nakashima, H.; Yamamoto, N.; Otaka, A.; Fujii, N. T140 analogs as CXCR4 antagonists identified as anti-metastatic agents in the treatment of breast cancer. *FEBS Lett.* **2003**, *550*, 79–83.
(9) Tsukada, N.; Burger, J. A.; Zvaifler, N. J.; Kipps, T. J. Distinctive features of "nurselike" cells that differentiate in the context of chronic lymphocytic leukemia. *Blood* **2002**, *99*, 1030–1037.
(10) Juarez, J.; Bradstock, K. F.; Gottlieb, D. J.; Bendall, L. J. Effects of inhibitors of the chemokine receptor CXCR4 on acute lymphoblastic leukemia cells in vitro. *Leukemia* **2003**, *17*, 1294–1300.
(11) Nanki, T.; Hayashida, K.; El–Gabalawy, H. S.; Suson, S.; Shi, K.; Girschick, H. J.; Yavuz, S.; Lipsky, P. E. Stromal cell-derived factor-1-CXC chemokine receptor interactions play a central role in CD4$^+$ T cell accumulation in rheumatoid arthritis synovium. *J. Immunol.* **2000**, *165*, 6590–6598.
(12) Tamamura, H.; Fujisawa, M.; Hiramatsu, K.; Mizumoto, M.; Nakashima, H.; Yamamoto, N.; Otaka, A.; Fujii, N. Identification of a CXCR4 antagonist, a T140 analog, as an anti-rheumatoid arthritis agent. *FEBS Lett.* **2004**, *569*, 99–104.
(13) Murakami, T.; Nakajima, T.; Koyanagi, Y.; Tachibana, K.; Fujii, N.; Tamamura, H.; Yoshida, N.; Waki, M.; Matsumoto, A.; Yoshie, O.; Kishimoto, T.; Yamamoto, N.; Nagasawa, T. A small molecule CXCR4 inhibitor that blocks T cell line-tropic HIV-1 infection. *J. Exp. Med.* **1997**, *186*, 1389–1393.
(14) Schols, D.; Struyf, S.; Van Damme, J.; Este, J. A.; Henson, G.; De Clercq, E. Inhibition of T-tropic HIV strains by selective antagonization of the chemokine receptor CXCR4. *J. Exp. Med.* **1997**, *186*, 1383–1388.
(15) Doranz, B. J.; Grovit-Ferbas, K.; Sharron, M. P.; Mao, S.-H.; Bidwell Goetz, M.; Daar, E. S.; Doms, R. W.; O'Brien, W. A. A small-molecule inhibitor directed against the chemokine receptor CXCR4 prevents its use as an HIV-1 coreceptor. *J. Exp. Med.* **1997**, *186*, 1395–1400.
(16) Donzella, G. A.; Schols, D.; Lin, S. W.; Este J. A.; Nagashima, K. A.; Maddon, P. J.; Allaway, G. P.; Sakmar, T. P.; Henson, G.; De Clercq, E.; Moore, J. P. AMD3100, a small molecule inhibitor of HIV-1 entry via the CXCR4 co-receptor. *Nat. Med.* **1998**, *4*, 72–77.
(17) Howard, O. M. Z.; Oppenheim, J. J.; Hollingshead, M. G.; Covey, J. M.; Bigelow, J.; McCormack, J. J.; Buckheit, R. W., Jr.; Clanton, D. J.; Turpin, J. A.; Rice, W. G. Inhibition of in vitro and in vivo HIV replication by a distamycin analogue that interferes with chemokine receptor function: A candidate for chemotherapeutic and microbicidal application. *J. Med. Chem.* **1998**, *41*, 2184–2193.
(18) Tamamura, H.; Xu, Y.; Hattori, T.; Zhang, X.; Arakaki, R.; Kanbara, K.; Omagari, A.; Otaka, A.; Ibuka, T.; Yamamoto, N.; Nakashima, H.; Fujii, N. A low molecular weight inhibitor against the chemokine receptor CXCR4: A strong anti-HIV peptide T140. *Biochem. Biophys. Res. Commun.* **1998**, *253*, 877–882.
(19) Tamamura, H.; Omagari, A.; Oishi, S.; Kanamoto, T.; Yamamoto, N.; Peiper, S. C.; Nakashima, H.; Otaka, A.; Fujii, N. Pharmacophore identification of a specific CXCR4 inhibitor, T140, leads to development of effective anti-HIV agents with very high selectivity indexes. *Bioorg. Med. Chem. Lett.* **2000**, *10*, 2633–2637.
(20) Fujii, N.; Oishi, S.; Hiramatsu, K.; Araki, T.; Ueda, S.; Tamamura, H.; Otaka, A.; Kusano, S.; Terakubo, S.; Nakashima, H.; Broach, J. A.; Trent, J. O.; Wang, Z.; Peiper, S. C. Molecular-size reduction of a potent CXCR4-chemokine antagonist using orthogonal combination of conformation- and sequence-based libraries. *Angew. Chem., Int. Ed.* **2003**, *42*, 3251–3253.
(21) Tamamura, H.; Fujii, N. Two Orthogonal Approaches to Overcome Multi-Drug Resistant HIV-1s: Development of Protease Inhibitors and Entry Inhibitors Based on CXCR4 Antagonists. *Curr. Drug Targets*—Infectious Disorders **2004**, *4*, 103–110.
(22) Ichiyama, K.; Yokoyama-Kumakura, S.; Tanaka, Y.; Tanaka, R.; Hirose, K.; Bannai, K.; Edamatsu, T.; Yanaka, M.; Niitani, Y.; Miyano-Kurosaki, N.; Takaku, H.; Koyanagi, Y.; Yamamoto, N. A duodenally absorbable CXC chemokine receptor 4 antagonist, KRH-1636, exhibits a potent and selective anti-HIV-1 activity. *Proc. Natl. Acad. Sci. U.S.A.* **2003**, *100*, 4185–4190.
(23) Tamamura, H.; Hiramatsu, K.; Ueda, S.; Wang, Z.; Kusano, S.; Terakubo, S.; Trent, J. O.; Peiper, S. C.; Yamamoto, N.; Nakashima, H.; Otaka, A.; Fujii, N. Stereoselective synthesis of [L-Arg,L/D-3-(2-naphthyl)alanine]-type (*E*)-alkene dipeptide isosteres and its application to the synthesis and biological evaluation of pseudopeptide analogs of the CXCR4 antagonist FC131. *J. Med. Chem.* **2005**, *48*, 380–391.
(24) Tamamura, H.; Araki, T.; Ueda, S.; Wang, Z.; Oishi, S.; Esaka, A.; Trent, J. O.; Nakashima, H.; Yamamoto, N.; Peiper, S. C.; Otaka, A.; Fujii, N. Identification of novel low molecular weight CXCR4 antagonists by structural tuning of cyclic tetrapeptide-scaffolds. *J. Med. Chem.* **2005**, *48*, 3280–3289.
(25) Ojida, A.; Mito-oka, Y.; Inoue, M.; Hamachi, I. First artificial receptors and chemosensors toward phosphorylated peptide in aqueous solution. *J. Am. Chem. Soc.* **2002**, *124*, 6256–6258.
(26) Mito-oka, Y.; Tsukiji, S.; Hiraoka, T.; Kasagi, N.; Shinkai, S.; Hamachi, I. Zn(II) dipicolylamine-based artificial receptor as a new entry for surface recognition of α-helical peptides in aqueous solution. *Tetrahedron Lett.* **2001**, *42*, 7059–7062.
(27) Ojida, A.; Inoue, M.; Mito-oka, Y.; Hamachi, I. Cross-linking strategy for molecular recognition and fluorescent sensing of a multi-phosphorylated peptide in aqueous solution. *J. Am. Chem. Soc.* **2003**, *125*, 10184–10185.
(28) Ojida, A.; Mito-oka, Y.; Sada, K.; Hamachi, I. Molecular recognition and fluorescence sensing of monophosphorylated peptides in aqueous solution by bis(zinc(II)-dipicolylamine)-based artificial receptors. *J. Am. Chem. Soc.* **2004**, *126*, 2454–2463.
(29) Abdel-Magid, A. F.; Maryanoff, C. A.; Carson, K. G. Reductive amination of aldehydes and ketones by using sodium triacetoxyborohydride. *Tetrahedron Lett.* **1990**, *31*, 5595–5598.
(30) Tamamura, H.; Hiramatsu, K.; Kusano, S.; Terakubo, S.; Yamamoto, N.; Trent, J. O.; Wang, Z.; Peiper, S. C.; Nakashima, H.; Otaka, A.; Fujii, N. Synthesis of potent CXCR4 inhibitors possessing low cytotoxicity and improved biostability based on T140 derivatives. *Org. Biomol. Chem.* **2003**, *1*, 3656–3662.
(31) Vallee, B. L.; Falchuk, K. H. The biochemical basis of zinc physiology. *Phys. Rev.* **1993**, *73*, 79–118.

JM060025U

JOC Article

Stereoselective Synthesis of 3,6-Disubstituted-3,6-dihydropyridin-2-ones as Potential Diketopiperazine Mimetics Using Organocopper-Mediated *anti*-S_N2' Reactions and Their Use in the Preparation of Low-Molecule CXCR4 Antagonists

Ayumu Niida,† Hiroaki Tanigaki,† Eriko Inokuchi,† Yoshikazu Sasaki,† Shinya Oishi,† Hiroaki Ohno,† Hirokazu Tamamura,† Zixuan Wang,‡ Stephen C. Peiper,‡ Kazuo Kitaura,† Akira Otaka,*,†,§ and Nobutaka Fujii*,†

Graduate School of Pharmaceutical Sciences, Kyoto University, Sakyo-ku, Kyoto 606-8501, Japan, Department of Pathology and Immunotherapy Center, Medical College of Georgia, Augusta, Georgia 30912, and Graduate School of Pharmaceutical Sciences, The University of Tokushima, Tokushima 770-8505, Japan

nfujii@pharm.kyoto-u.ac.jp; aotaka@ph.tokushima-u.ac.jp

Received February 24, 2006

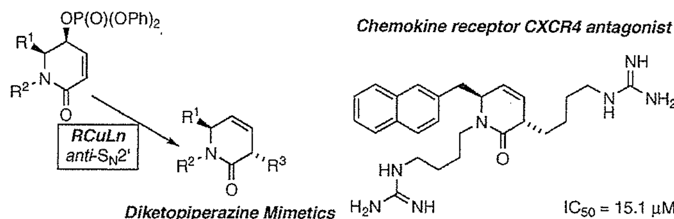

Organocopper-mediated *anti*-S_N2' reactions of γ-phosphoryloxy-α,β-unsaturated-δ-lactams were used to prepare highly functionalized diketopiperazine mimetics. The substrate phosphates **24**, **32**, and **47** were prepared from α-amino acid-derived allylic alcohols **10** by a sequence of reactions that included ring-closing metathesis. In the reactions of phosphates with organocopper reagents, the addition of LiCl dramatically improved *anti*-S_N2' selectivity, indicating that an organocopper cluster containing lithium chloride plays an important role in the determination of regioselectivity. This reaction system was applied to the preparation of novel low molecular weight CXCR4-chemokine receptor antagonists.

Introduction

The replacement of a peptide bond in biologically active peptides with a non-hydrolyzable unit is a promising approach for peptide-lead drug discovery. (*E*)-Alkene dipeptide isosteres (EADIs) represent amide-bond mimetics that possess excellent structural homology and resistance to proteases.[1] Over the past decade, we have engaged in the development of efficient stereoselective methodology for the preparation of EADIs utilizing organocopper-mediated transformations along with their application to biologically active peptides.[2,3] Piperazine-2,5-dione (diketopiperazine: DKP) derivatives **1** represent the smallest cyclic peptides consisting of two α-amino acid residues. This well-organized structure is widely seen in compounds of biological or medicinal interest. Therefore, it seemed logical that the DKP nucleus could serve as a drug template with appropriately arrayed pharmacophores (Figure 1).[4] On the basis of our studies on EADIs, we envisioned that the replacement of a DKP *cis*-amide bond with structurally similar (*Z*)-alkene units could provide DKP mimetics **2** as novel starting points for creating drug-like structures (Figure 2).

* Corresponding Authors. Phone: +81-75-753-4551 (N.F.); +81-88-633-7283 (A.O.). Fax: +81-75-753-4570 (N.F.); +81-88-633-9505 (A.O.).
† Kyoto University.
‡ Medical College of Georgia.
§ The University of Tokushima.

(1) For alkene dipeptide isosteres, see: (a) Christos, T. E.; Arvanitis, A.; Cain, G. A.; Johnson, A. L.; Pottorf, R. S.; Tam, S. W.; Schmidt, W. K. *Bioorg. Med. Chem. Lett.* **1993**, *3*, 1035. (b) Bohnstedt, A. C.; Prasad, J. V. N. V.; Rich, D. H. *Tetrahedron Lett.* **1993**, *34*, 5217. (c) Wai, J. S.; Bamberger, D. L.; Fisher, T. E.; Graham, S. L.; Smith, R. L.; Gibbs, J. B.; Mosser, S. D.; Oliff, A. I.; Pompliano, D. L.; Rands, E.; Kohl, N. E. *Bioorg. Med. Chem.* **1994**, 2, 939. (d) Vasbinder, M. M.; Jarvo, E. R.; Miller, S. J. *Angew. Chem., Int. Ed.* **2001**, *40*, 2824. (e) Wipf, P.; Xiao, J. *Org. Lett.* **2005**, *7*, 103. (f) Jenkins, C. L.; Vasbinder, M. M.; Miller, S. J.; Raines, R. T. *Org. Lett.* **2005**, *7*, 2619.

10.1021/jo060390t CCC: $33.50 © 2006 American Chemical Society
Published on Web 04/21/2006

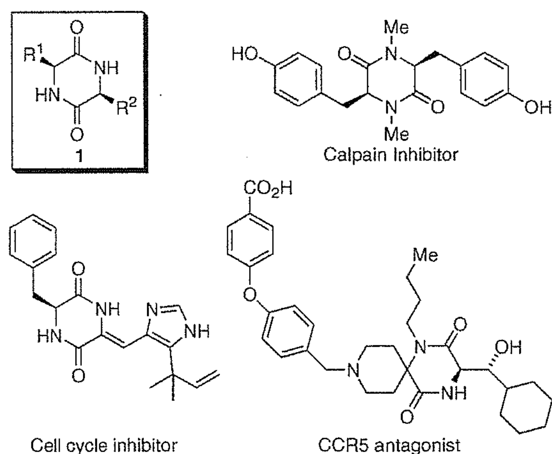

FIGURE 1. General structure of 2,5-diketopiperazine and biologically active derivatives.

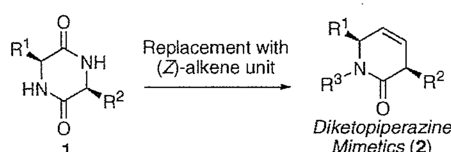

FIGURE 2. Design of diketopiperazine mimetics.

However, to our knowledge, there have been only a few reports in which 3,6-disubstituted-3,6-dihydropyridin-2-ones (DKP mimetics **2**) having side-chain functionalities have been synthesized in stereoselective fashions. These include synthetic protocols that employ the ring-closing metathesis or palladium-catalyzed carbonylation as key reactions (Scheme 1). Ring-closing metathesis of bisolefinic amide **5** with Grubbs' ruthenium alkylidene complexes yielded the desired DKP mimetics **2**, where the stereochemical outcome depends on the stereochemistry of the requisite metathesis substrate **5**, which was obtained by coupling between enantiomerically pure 1-substituted prop-2-enylamines **3** and 2-substituted but-3-enoic acids **4**.[5] Alternatively, Knight et al. have reported the enantioselective synthesis of 3,6-dihydro-1*H*-pyridin-2-ones **7** by Pd-catalyzed decarboxylative carbonylation of 5-vinyloxazolidin-2-ones **6**,

SCHEME 1. Previous Synthetic Routes for the Preparation of Diketopiperazine Mimetics

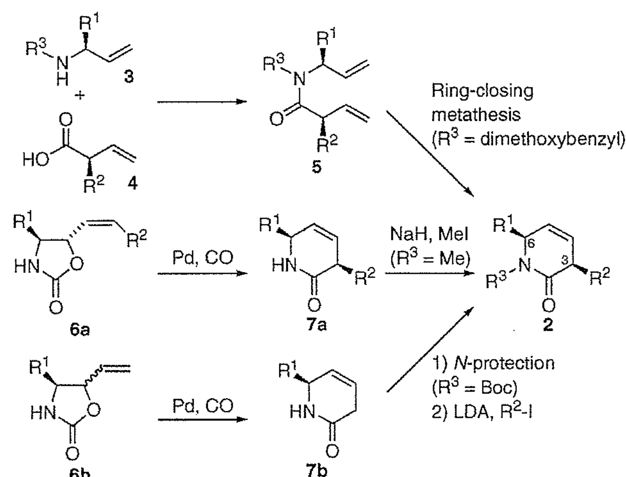

SCHEME 2. Retrosynthetic Analysis of Diketopiperazine Mimetics Prepared by an Organocopper-Mediated *anti*-S_N2' Reaction[a]

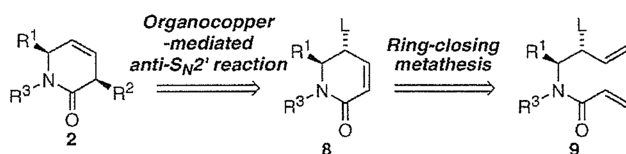

[a] L = leaving group.

which were synthesized from the corresponding α-amino aldehydes.[6] The stereochemistry at the 6-position was derived from that of the precursor α-amino aldehyde. The stereoselective introduction of substituents at the 3-position was achieved in two ways. One way involves the Pd-catalyzed reaction of 5-(alk-1-enyl)oxazolidinones **6a** to provide 3,6-disubstituted analogues **7a**;[6a,b] however, this requires long reaction times, and the product yields were rather low. To circumvent these problems, a two-step protocol consisting of the Pd-catalyzed synthesis of the 6-substituted pyridinones **7b** followed by an enolate alkylation (**7b** to **2**) was developed.[6c] In this methodology, the nature of both the electrophiles incoming to the enolate and the substituent on the nitrogen affect the diastereoselection at the 3-position.

Our approach for the stereoselective preparation of DKP mimetics **2** is shown in Scheme 2. We envisioned that the γ-activated-α,β-unsaturated lactams **8** could be converted into the corresponding dihydropyridinone derivatives **2** by an organocopper-mediated *anti*-S_N2' reaction. A Ru-catalyzed olefin metathesis[7] reaction is suitable for the synthesis of key substrates

(2) (a) Ibuka, T.; Habashita, H.; Funakoshi, S.; Fujii, N.; Oguchi, Y.; Uyehara, T.; Yamamoto, Y. *Angew. Chem., Int. Ed. Engl.* **1990**, *29*, 801. (b) Ibuka, T.; Habashita, H.; Otaka, A.; Fujii, N.; Oguchi, Y.; Uyehara, T.; Yamamoto, Y. *J. Org. Chem.* **1991**, *56*, 4370. (c) Ibuka, T.; Nakai, K.; Habashita, H.; Hotta, Y.; Fujii, N.; Mimura, N.; Miwa, Y.; Taga, T.; Yamamoto, Y. *Angew. Chem., Int. Ed. Engl.* **1994**, *33*, 652. (d) Oishi, S.; Tamamura, H.; Yamashita, M.; Odagaki, Y.; Hamanaka, N.; Otaka, A.; Fujii, N. *J. Chem. Soc., Perkin Trans. 1* **2001**, 2445. (e) Oishi, S.; Niida, A.; Kamano, T.; Miwa, Y.; Taga, T.; Odagaki, Y.; Hamanaka, N.; Yamamoto, M.; Ajito, K.; Tamamura, H.; Otaka, A.; Fujii, N. *J. Chem. Soc., Perkin Trans. 1* **2002**, 1786.

(3) (a) Fujimoto, K.; Doi, R.; Hosotani, R.; Wada, M.; Lee, J.-U.; Koshiba, T.; Ibuka, T.; Habashita, H.; Nakai, K.; Fujii, N.; Imamura, M. *Life Sci.* **1997**, *60*, 29. (b) Kawaguchi, M.; Hosotani, R.; Ohishi, S.; Fujii, N.; Tulachan, S. S.; Koizumi, M.; Toyoda, E.; Masui, T.; Nakajima, S.; Tsuji, S.; Ida, J.; Fujimoto, K.; Wada, M.; Doi, R.; Imamura, M. *Biochem. Biophys. Res. Commun.* **2001**, *288*, 711. (c) Tamamura, H.; Hiramatsu, K.; Miyamoto, K.; Omagari, A.; Oishi, S.; Nakashima, H.; Yamamoto, N.; Kuroda, Y.; Nakagawa, T.; Otaka, A.; Fujii, N. *Bioorg. Med. Chem. Lett.* **2002**, *12*, 923. (d) Oishi, S.; Kamano, T.; Niida, A.; Odagaki, Y.; Hamanaka, N.; Yamamoto, M.; Ajito, K.; Tamamura, H.; Otaka, A.; Fujii, N. *J. Org. Chem.* **2002**, *67*, 6162. (e) Tamamura, H.; Koh, Y.; Ueda, S.; Sasaki, Y.; Yamasaki, T.; Aoki, M.; Maeda, K.; Watai, Y.; Arikuni, H.; Otaka, A.; Mitsuya, H.; Fujii, N. *J. Med. Chem.* **2003**, *46*, 1764. (f) Tamamura, H.; Hiramatsu, K.; Ueda, S.; Wang, Z.; Kusano, S.; Terakubo, S.; Trent, J. O.; Peiper, S. C.; Yamamoto, N.; Nakashima, H.; Otaka, A.; Fujii, N. *J. Med. Chem.* **2005**, *48*, 380.

(4) (a) Kanoh, K.; Kohno, S.; Katada, J.; Takahashi, J.; Uno, I.; Hayashi, Y. *Bioorg. Med. Chem.* **1999**, *7*, 1451. (b) Donkor, I. O.; Sanders, M. L. *Bioorg. Med. Chem. Lett.* **2001**, *11*, 2647. (c) Maeda, K.; Nakata, H.; Koh, Y.; Miyakawa, T.; Ogata, H.; Takeoka, Y.; Shibayama, S.; Sagawa, K.; Fukushima, D.; Moravek, J.; Koyanagi, Y.; Mitsuya, H. *J. Virol.* **2004**, *78*, 8654. (d) Nam, N.-H.; Ye, G.; Sun, G.; Parang, K. *J. Med. Chem.* **2004**, *47*, 3131. (e) Borthwick, A. D.; Davies, D. E.; Exall, A. M.; Livermore, D. G.; Sollis, S. L.; Nerozzi, F.; Allen, M. J.; Perren, M.; Shabbir, S. S.; Woollard, P. M.; Wyatt, P. G. *J. Med. Chem.* **2005**, *48*, 6956.

(5) (a) Boucard, V.; Sauriat-Dorizon, H.; Guibé, F. *Tetrahedron* **2002**, *58*, 7275. (b) Humphries, M. E.; Murphy, J.; Phillips, A. J.; Abell, A. D. *J. Org. Chem.* **2003**, *68*, 2432.

(6) (a) Knight, J. G.; Ainge, S. W.; Harm, A. M.; Harwood, S. J.; Maughan, H. I.; Armour, D. R.; Hollinshead, D. M.; Jaxa-Chamiec, A. A. *J. Am. Chem. Soc.* **2000**, 122, 2944. (b) Knight, J. G.; Tchabanenko, K. *Tetrahedron* **2002**, *58*, 6659. (c) Anderson, T. F.; Knight, J. G.; Tchabanenko, K. *Tetrahedron Lett.* **2003**, *44*, 757.

8, in terms of compatibility with various functional groups.[8] The amide nitrogen should be appropriately protected by a group such as Me or dimethoxybenzyl (DMB) to raise the proportion of conformers with *cis*-amide geometry, which is necessary for facile olefin metathesis.[9] We present herein the efficient conversion of γ-oxygenated-α,β-unsaturated-δ-lactams **8** to DKP mimetics **2** using organocopper-mediated *anti*-S_N2' reactions. This novel methodology was applied to the synthesis of low molecular weight CXCR4 antagonists on the basis of the DKP mimetic structure.[10]

Results and Discussion

Our synthesis started from the known *N*-Ns-*O*-TBS protected *syn*-1,2-amino alcohol *syn*-**11**[11] (Ns: 2-nitrobenzenesulfonyl; TBS: *tert*-butyldimethylsilyl) derived from allylic alcohol *syn*-**10**[12] (Scheme 3). The silyl ether *syn*-**11** was subjected to *N*-modification either with MeI, K_2CO_3, or with DMB−OH, Ph_3P, and DEAD (Mitsunobu conditions) to afford *N*-Me **12a** and *N*-DMB **12b** derivatives, respectively.[13] After removal of the Ns group of **12** by treatment with thiolate anion under basic conditions, the resulting secondary amines were acylated with acryloyl chloride to yield the metathesis substrates **13**. The corresponding diastereomer **13c** was synthesized from *N*-Boc protected *anti*-1,2-amino alcohol *anti*-**10**[12] by a sequence of reactions identical to those used for the preparation of **13a**. Nonalkylated derivative **13d** was also synthesized.

The attempted olefin metathesis of **13a−c** with Grubbs' Ru catalyst **A**[14] resulted in low cyclization yields (Table 1, entries 1−4). The use of the second-generation catalyst **B**[15] improved the yields (entries 5−7), although long reaction times under reflux were required. Ring-closing metathesis of **13** with catalyst **B** gave the benzylidene derivative **15** as a side product. This prompted us to postulate that the low reactivity of the substrates may be partly attributed to the presence of the bulky TBS group. Therefore, TBS-deprotected derivatives **16a−c**, obtained in high yields by the treatment of **13a−c** with TBAF (88−99%), were subjected to the metathesis reaction with catalyst **A** or **B** (Table 2). Although the reaction with catalyst **A** did not afford satisfactory results (entries 1 and 2), ring-closure with catalyst **B** proceeded smoothly at room temperature to yield the desired cyclized compounds **17a−c** in good yields (entries 3−6). Even for substrate **13d**, which lacked an *N*-alkyl substituent, the catalyst **B** afforded the cyclized product **17d** in a moderate yield (entry 7).

SCHEME 3. Synthesis of Requisite Substrates for Ring-Closing Metathesis[a]

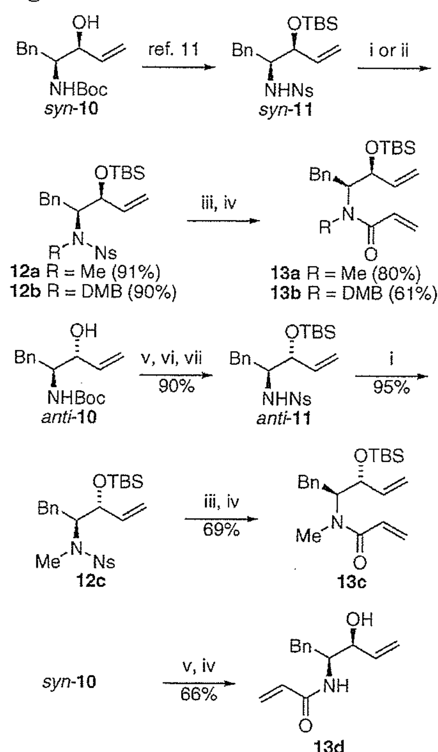

[a] Reagents and conditions: (i) MeI, K_2CO_3, DMF; (ii) DMB-OH, PPh_3, DEAD, THF; (iii) $HSCH_2CO_2H$, LiOH, DMF; (iv) CH_2=CHCOCl, Et_3N, CH_2Cl_2; (v) 4 M HCl in dioxane; (vi) Ns-Cl, 2,4,6-collidine, $CHCl_3$; (vii) TBSOTf, 2,6-lutidine, CH_2Cl_2.

TABLE 1. Ring-Closing Metathesis of *O*-TBS-Protected Acrylamide Derivatives

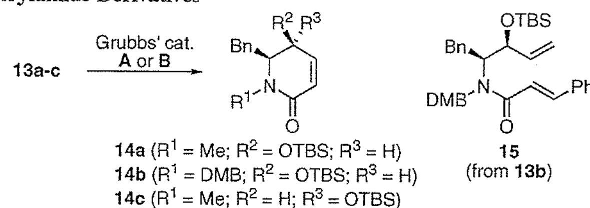

entry	substrate	cat. (equiv)	conditions[a]	product[b,c] (yield, %)
1	**13a**	**A** (0.6)	rt, 48 h	**14a** (trace)
2	**13a**	**A** (0.6)	reflux, 36 h	**14a** (37)
3	**13b**	**A** (0.1)	reflux, 36 h	**14b** (10)
4	**13c**	**A** (0.6)	reflux, 36 h	**14c** (30)
5	**13a**	**B** (0.6)	rt, 36 h	**14a** (57)
6	**13a**	**B** (0.6)	reflux, 48 h	**14a** (61)
7	**13b**	**B** (0.6)	reflux, 36 h	**14b** (29)

[a] CH_2Cl_2 was used as solvent. [b] Isolated yield. [c] Starting materials were recovered, except for entry 6.

(7) (a) Yet, L. *Chem. Rev.* **2000**, *100*, 2963. (b) Trnka, T. M.; Grubbs, R. H. *Acc. Chem. Res.* **2001**, *34*, 18. (c) Deiters, A.; Martin, S. F. *Chem. Rev.* **2004**, *104*, 2199.

(8) (a) Gao, Y.; Wei, C.-Q.; Burke, T. R., Jr. *Org. Lett.* **2001**, *3*, 1617. (b) Stymiest, J. L.; Mitchell, B. F.; Wong, S.; Vederas, J. C. *Org. Lett.* **2003**, *5*, 47. (c) Walensky, L. D.; Kung, A. L.; Escher, I.; Malia, T. J.; Barbuto, S.; Wright, R. D.; Wagner, G.; Verdine, G. L.; Korsmeyer, S. J. *Science* **2004**, *305*, 1466. (d) Tamamura, H.; Araki, T.; Ueda, S.; Wang, Z.; Oishi, S.; Esaka, A.; Trent, J. O.; Nakashima, H.; Yamamoto, N.; Peiper, S. C.; Otaka, A.; Fujii, N. *J. Med. Chem.* **2005**, *48*, 3280.

(9) Rutjes, F. P. J. T.; Schoemaker, H. E. *Tetrahedron Lett.* **1997**, *38*, 677.

(10) A portion of this work has appeared in preliminary communications: (a) Niida, A.; Mizumoto, M.; Sasaki, Y.; Tamamura, H.; Otaka, A.; Fujii, N. In *Peptide Science*; Shimohigashi, Y., Ed.; The Japanese Peptide Society: Osaka, 2004; p 169. (b) Niida, A.; Oishi, S.; Sasaki, Y.; Mizumoto, M.; Tamamura, H.; Fujii, N.; Otaka, A. *Tetrahedron Lett.* **2005**, *46*, 4183.

(11) Niida, A.; Tomita, K.; Mizumoto, M.; Tanigaki, H.; Terada, T.; Oishi, S.; Otaka, A.; Inui, K.; Fujii, N. *Org. Lett.* **2006**, *8*, 616.

(12) Hanson, G. J.; Lindberg, T. *J. Org. Chem.* **1985**, *50*, 5399.

(13) (a) Fukuyama, T.; Jow, C.-K.; Cheung, M. *Tetrahedron Lett.* **1995**, *36*, 6373. (b) Hidai, Y.; Kan, T.; Fukuyama, T. *Chem. Pharm. Bull.* **2000**, *48*, 1570. (c) Lin, X.; Dorr, H.; Nuss, J. M. *Tetrahedron Lett.* **2000**, *41*, 3309.

(14) Grubbs, R. H.; Chang, S. *Tetrahedron* **1998**, *54*, 4413.

(15) (a) Scholl, M.; Ding, S.; Lee, C. W.; Grubbs, R. H. *Org. Lett.* **1999**, *1*, 953. (b) Arisawa, M.; Theeraladanon, C.; Nishida, A.; Nakagawa, M. *Tetrahedron Lett.* **2001**, *42*, 8029.

TABLE 2. Ring-Closing Metathesis of Acrylamides Containing Allylic Alcohol Moieties

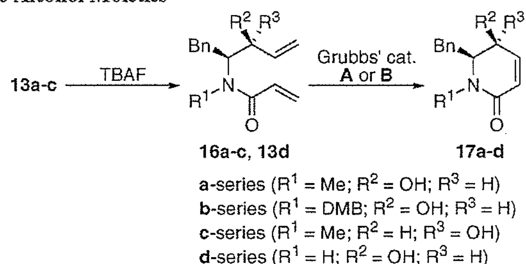

entry	substrate	cat. (equiv)	conditions[a]	product[b] (yield, %)
1	**16a**	**A** (0.15)	rt, 12 h	**17a** (trace)[c]
2	**16b**	**A** (0.15)	reflux, 12 h	**17b** (31)[c]
3	**16a**	**B** (0.15)	rt, 12 h	**17a** (74)
4	**16a**	**B** (0.05)	rt, 6 h	**17a** (84)
5	**16b**	**B** (0.15)	rt, 12 h	**17b** (74)
6	**16c**	**B** (0.15)	rt, 12 h	**17c** (84)
7	**13d**	**B** (0.15)	rt, 12 h	**17d** (53)

[a] CH_2Cl_2 was used as solvent. [b] Isolated yield. [c] Starting materials were recovered.

SCHEME 4. Attempted Conversion of 17a to γ-Activated Derivatives Followed by Organocopper-Mediated Reactions[a]

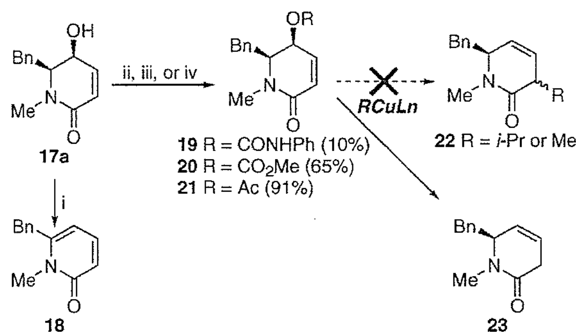

[a] Reagents and conditions: (i) MsCl, pyridine, CH_2Cl_2; (ii) $ClCO_2Me$, DMAP, pyridine, CH_2Cl_2; (iii) PhNCO, BF_3·Et_2O, Et_2O; (iv) Ac_2O, DMAP, pyridine, $CHCl_3$. RCuLn: see text.

Next, we examined the activation of the γ-hydroxyl group of **17a** (Scheme 4). Generally, the use of γ-mesyloxy groups is suitable for the organocopper-mediated reaction of acyclic (*E*)-α,β-enoates to prepare EADIs in satisfactory yield.[2] However, the reaction of **17a** with Ms-Cl-pyridine resulted in the formation of the pyridinone derivative **18**. Thus, we examined alternative substrates having a less electron-withdrawing *O*-activating group, including carbonate,[16] carbamate,[17] and acetate[18] derivatives. These compounds were obtained in low to excellent yields (carbamate **19**, 10%; carbonate **20**, 65%; acetate **21**, 91%). However, attempted reactions of these compounds with organocopper reagents [*i*-PrCu(CN)MgCl·BF_3·2LiCl or *i*-Pr_2Cu-(CN)$(MgCl)_2$·BF_3·2LiCl][2e] for the preparation of S_N2' alkylation product **22** led to the recovery of starting materials along with the formation of the undesired reduced product **23**. The treatment of the easily obtainable acetate **21** with Gilman-type (Me_2CuLi_2·LiI·2LiBr) and "higher-order" (Me_3CuLi_2·LiI·3LiBr) cuprate gave the reduction product **23** in 42 and 82% yields, respectively, without the formation of the desired *anti*-S_N2' product. The use of "lower-order" organocopper reagent (MeCu·LiI·LiBr) resulted in 86% recovery of the starting material.

TABLE 3. Organocopper-mediated Reactions of γ-Phosphoryloxy-α,β-unsaturated-δ-lactam 24

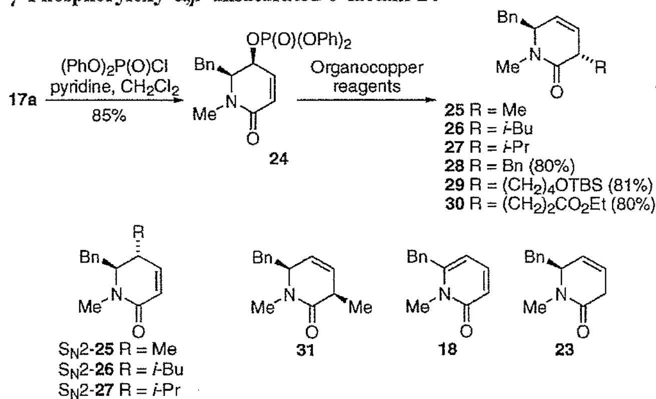

entry	organocopper reagent[a,b,c]	product(s) (isolated yield, %)
1	Me_3CuLi_2·LiI·3LiBr	**25** (35), S_N2-**25** (10), **31** (3), **23** (23)
2	Me_2CuLi·LiI·2LiBr	**25** (67), S_N2-**25** (8), **31** (5), **23** (5)
3	MeCu·LiI·LiBr	**25** (83)
4	MeCuI·MgCl	**25** (24), S_N2-**25** (40)
5	MeCuI·MgCl·2LiCl	**25** (93)
6	MeCu(CN)·MgCl·2LiCl	**25** (77), S_N2-**25** (trace)
7	MeCu(CN)·MgCl·2LiCl·BF_3	**25** (55), S_N2-**25** (7)
8	$Me_2Cu(CN)$·$(MgCl)_2$·2LiCl·BF_3	S_N2-**25** (11), **23** (17)
9	*i*-BuCu·2LiI[d]	**26** (63), S_N2-**26** (13)
10	*i*-BuCu·2LiI·2LiCl[d]	**26** (82)
11	*i*-PrCuI·MgCl·2LiCl[e]	**27** (trace), S_N2-**27** (trace), **18** (62)
12	*i*-PrCu(CN)·MgCl·2LiCl	**27** (84), S_N2-**27** (8)
13	*i*-PrCu(CN)·MgCl·2LiCl·BF_3	**27** (59), S_N2-**27** (12)
14	*i*-PrCu(CN)·MgCl·2LiCl·5BF_3	**27** (36), S_N2-**27** (45)

[a] Two equivalents of reagents were used, except for entry 8 (4 equiv). [b] THF or a mixed solvent consisting of THF and Et_2O (or Et_2O−*n*-pentane) was used. [c] Reactions were carried out at −78 °C for 20 min, except for entry 11. [d] Alkyllithium for the preparation of the organocopper reagent was obtained from the reaction of the corresponding alkyl iodide and a pentane solution of *tert*-butyllithium (See the Supporting Information). [e] Reaction at −78 °C for 20 min then at 0 °C for 40 min.

Because allylic phosphates have also been documented to undergo highly stereoselective *anti*-S_N2' reactions with organocopper reagents,[19] we next examined the feasibility of using γ-phosphoryloxy-α,β-unsaturated-δ-lactams for the preparation of disubstituted DKP mimetics (Table 3). The reaction of **17a** with diphenylphosphoryl chloride in the presence of pyridine proceeded smoothly to give the phosphate derivative **24** in 85% yield as an activated compound, which was stable below 4 °C. Upon standing at room temperature, the phosphates were gradually converted to the pyridinone derivative **18**.

First, the reaction of phosphate **24** with MeLi·LiBr complex-derived organocopper-reagents was investigated. Contrary to the finding that the reaction of acetate **21** with MeLi·LiBr-derived reagents did not afford any S_N2' alkylated product, the phosphate **24** was converted into mixtures containing the desired *anti*-

(16) (a) Boquel, P.; Chapleur, Y. *Tetrahedron Lett.* **1990**, *31*, 1869. (b) Kang, S.-K.; Park, Y.-W.; Lee, D.-H.; Sim, H.-S.; Jeon, J.-H. *Tetrahedron: Asymmetry* **1992**, *3*, 705. (c) Spino, C.; Tremblay, M.-C.; Gobdout, C. *Org. Lett.* **2004**, *6*, 2801. (d) Spino, C.; Allan, M. *Can. J. Chem.* **2004**, *82*, 177.

(17) (a) Gallina, C.; Ciattini, P. G. *J. Am. Chem. Soc.* **1979**, *101*, 1035. (b) Denmark, S. E.; Marble, L. K. *J. Org. Chem.* **1990**, *55*, 1984. (c) Smitrovich, J. H.; Woerpel, K. A. *J. Org. Chem.* **2000**, *65*, 1601. (d) Peng, Z.-H.; Woerpel, K. A. *Org. Lett.* **2001**, *3*, 675.

(18) (a) Goering, H. L.; Singleton, V. D., Jr. *J. Am. Chem. Soc.* **1976**, *98*, 7854. (b) Goering, H. L.; Singleton, V. D., Jr. *J. Org. Chem.* **1983**, *48*, 1531. (c) Belelie, J. L.; Chong, J. M. *J. Org. Chem.* **2002**, *67*, 3000.

S_N2' product in varying ratios, depending on the organocopper reagents employed (Table 3, entries 1 and 2). It should be noted that the reaction of **24** with MeCu·LiI·LiBr in THF–Et_2O at −78 °C for 20 min proceeded smoothly to afford **25** in 83% isolated yield, without other accompanying products (Table 3, entry 3).[20]

On the basis of these results, we speculated that "lower-order" reagent systems such as MeCu·MX, prepared from a 1:1 mixture of organometallic reagent and copper salt, affected the *anti*-S_N2' conversion of the phosphate. Being encouraged by these results, we next examined Grignard reagent (MeMgCl) as an alkyl source for the organocopper reagents. Unexpectedly, the treatment of phosphate **24** with MeCuI·MgCl, formed from equimolar amounts of MeMgCl and CuI, gave a mixture of S_N2 (S_N2-**25**: 40%) and *anti*-S_N2'(**25**: 24%) products (Table 3, entry 4). In contrast, the addition of the lithium salts (LiCl) dramatically improved the selectivity to produce the desired *anti*-S_N2' compound **25** in 93% isolated yield (Table 3, entry 5). This indicated that using "lower-order" reagents in the presence of lithium salts provides a suitable system for the *anti*-S_N2' reaction of γ-phosphoryloxy-α,β-unsaturated-δ-lactams. Recently, a mixture of CuCN and LiCl (1:2, mole ratio), which is a soluble copper complex in THF, was successfully applied to a wide range of organocopper-mediated transformations.[21] In our present work, the use of a CuCN·2LiCl complex gave the desired compound **25** in 77% yield with an accompanying small amount of S_N2 product (Table 3, entry 6). It is well-documented that the addition of Lewis acids such as BF_3·Et_2O or TMSCl to organocopper-mediated reactions improves the chemical yields or regioselectivity.[22] However, inclusion of BF_3·Et_2O in the CuCN-mediated reaction of the phosphate **24** led to an increase in S_N2 product (Table 3, entry 7). The corresponding reaction with "higher order" cyanocuprate–BF_3 [$Me_2Cu(CN)\cdot(MgCl)_2\cdot 2LiCl\cdot BF_3$] was unsuccessful, resulting in a complex mixture without formation of the desired *anti*-S_N2' product (Table 3, entry 8).

Next, the introduction of other alkyl groups using various organometallic reagents was investigated. The reaction of phosphate **24** with organocopper reagents prepared from *i*-BuLi and CuI (1:1 ratio) gave the desired *anti*-S_N2' product **26** (63% yield) along with a small amount of S_N2-**26** (13%; Table 3, entry 9). As expected, the addition of LiCl to *i*-BuCu·2LiI completely suppressed the formation of S_N2-**26** (Table 3, entry 10). In sharp contrast, the reaction with the copper reagent derived from *i*-PrMgCl and CuI did not proceed at −78 °C. When the reaction was conducted at room temperature, pyridinone derivative **18** was obtained in 62% isolated yield (Table 3, entry 11). This was probably due both to steric hindrance and to higher basicity of the reagent having a secondary carbon center. On the other hand, use of CuCN·2LiCl in combination with *i*-PrMgCl afforded the desired *anti*-S_N2' product **27** (Table 3, entry 12). Generally, CuCN-based reagents have been reported to exhibit higher soft nucleophilic character than reagents prepared using other copper salts including CuI.[23] These may be more suitable for S_N2' reactions of **24** with the copper reagents having an *i*-Pr group. An increased formation of the S_N2 product was observed when the reaction with *i*-PrCu(CN)·MgCl·2LiCl was conducted in the presence of BF_3·Et_2O (Table 3, entries 13 and 14), as in the case of MeCu(CN)·MgCl·2LiCl. Other diketopiperazine mimetics **28–30**, containing phenyl, hydroxyl, and ester functional groups, respectively, were also synthesized by use of organocopper-mediated *anti*-S_N2' reactions.[10] We have confirmed that organocopper-mediated reactions of 5,6-*trans*-phosphate **32** derived from lactam **17c** proceeded smoothly in an *anti*-S_N2' manner to yield 3,6-*cis*-diketopiperazine mimetics **33–38** (Scheme 5).[10,24] In all cases, no detectable amounts of S_N2 products were observed. This is probably due to the presence of a benzyl group, which effectively prevents the access of organocopper reagent to the γ-position from the opposite side of the leaving group.

SCHEME 5. Organocopper-Mediated *anti*-S_N2' Reaction of 5,6-*trans*-Phosphate 32

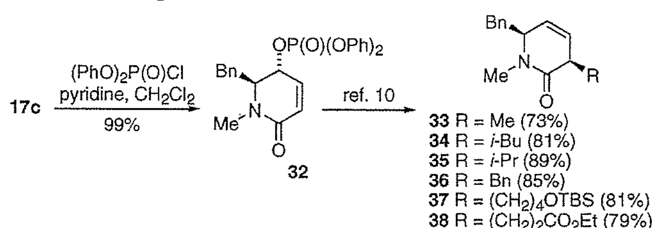

The involvement of lithium salts is likely to be crucial for the preferential formation of *anti*-S_N2' products (e.g., Table 3, entry 4 vs 5). We hypothesized that cluster-like structures consisting of organocopper and lithium salts were responsible for determining regioselectivity. The importance of cluster structures of organocopper and lithium salts is well-documented in organocopper chemistry.[25] Of note, in conjugate additions to α,β-unsaturated carbonyl compounds using organocuprates, including Me_2CuLi·LiX (X = I or CN), a "trap and bite" mechanism has been postulated and supported by theoretical investigations (Figure 3).[26] According to this mechanism, organocuprate cluster reagent **39** traps the substrate by coordinating with a carbonyl group, followed by the opening of the cluster to form the "biting" structure **40**. This results in C–C bond formation by subsequent reductive elimination. It has been

(19) (a) Yanagisawa, A.; Noritake, Y.; Nomura, N.; Yamamoto, H. *Synlett* **1991**, 251. (b) Yanagisawa, A.; Nomura, N.; Yamamoto, H. *Synlett* **1991**, 513. (c) Arai, M.; Lipshutz, B. H.; Nakamura, E. *Tetrahedron* **1992**, *48*, 5709. (d) Yanagisawa, A.; Nomura, N.; Yamamoto, H. *Tetrahedron* **1994**, *50*, 6017. (e) Torneiro, M.; Fall, Y.; Castedo, L.; Mouriño, A. *J. Org. Chem.* **1997**, *62*, 6344. (f) Belelie, J. L.; Chong, J. M. *J. Org. Chem.* **2001**, *66*, 5552. (g) Calaza, M. I.; Hupe, E.; Knochel, P. *Org. Lett.* **2003**, *5*, 1059. (h) Dieter, R. K.; Gore, V. K.; Chen, N. *Org. Lett.* **2004**, *6*, 763. (i) Soorukram, D.; Knochel, P. *Org. Lett.* **2004**, *6*, 2409.

(20) Generally, an increase in MeLi, a copper salt ratio, improved the electron-donating activity of the reagents. The reactivity of MeLi-derived organocopper reagents toward the acetate **21** reflects this nature. Organocopper reagents possessing highly reducing potency proved to be unsuitable for the *anti*-S_N2' reaction of the phosphate **24**. See: Chounan, Y.; Horino, H.; Ibuka, T.; Yamamoto, Y. *Bull. Chem. Soc. Jpn.* **1997**, *70*, 1953.

(21) (a) Swenson, R. E.; Sowin, T. J.; Zhang, H. Q. *J. Org. Chem.* **2002**, *67*, 9182. (b) Harrington-Frost, N.; Leuser, H.; Calaza, M. I.; Kneisel, F. F.; Knochel, P. *Org. Lett.* **2003**, *5*, 2111. (c) Hupe, E.; Calaza, M. I.; Knochel, P. *Chem.—Eur. J.* **2003**, *9*, 2789. (d) Kobayashi, Y.; Nakata, K.; Ainai, T. *Org. Lett.* **2005**, *7*, 183.

(22) (a) Yamamoto, Y.; Yamamoto, S.; Yatagai, H.; Maruyama, K. *J. Am. Chem. Soc.* **1980**, *102*, 2318. (b) Yamamoto, Y.; Yamamoto, S.; Yatagai, H.; Ishihara, Y.; Maruyama, K. *J. Org. Chem.* **1982**, *47*, 119. (c) Lipshutz, B. H.; Ellsworth, E. L.; Siahaan, T. J. *J. Am. Chem. Soc.* **1989**, *111*, 1351. (d) Ibuka, T.; Tanaka, M.; Nishii, S.; Yamamoto, Y. *J. Am. Chem. Soc.* **1989**, *111*, 4864. (e) Horiguchi, Y.; Komatsu, M.; Kuwajima, I. *Tetrahedron Lett.* **1989**, *30*, 7087. (f) Cardillo, G.; Gentilucci, L.; Tolomelli, A.; Tomasini, C. *Tetrahedron* **1999**, *55*, 6231.

(23) Ibuka, T.; Tanaka, M.; Nemoto, H.; Yamamoto, Y. *Tetrahedron* **1989**, *45*, 435.

(24) Relative configurations of the resulting DKP mimetics **25–30** and **32–37** were determined based on X-ray and ^1H NMR analyses. In ^1H NMR measurements, upfield shifts of α-protons of 3,6-trans derivatives, which were probably caused by an anisotropic effect of the side-chain phenyl ring, were observed (see the Supporting Information).

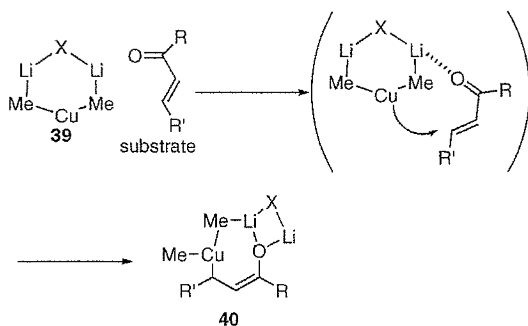

FIGURE 3. Conjugate addition of organocuprates to α,β-unsaturated carbonyl compounds via a "trap and bite" mechanism.

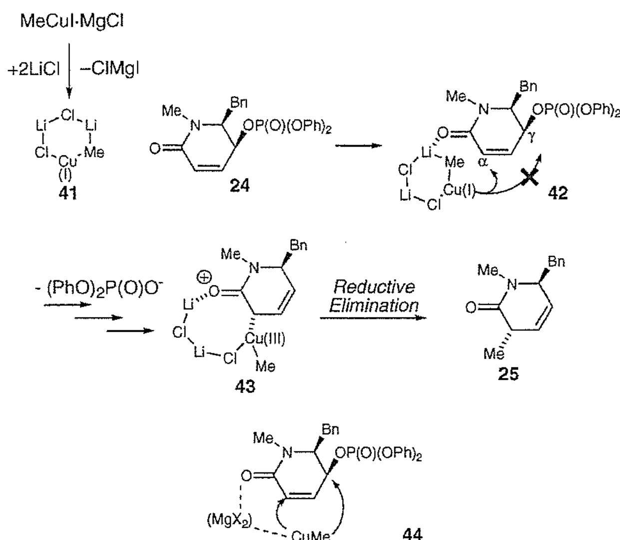

FIGURE 4. Potential mechanism for *anti*-S_N2' selectivity induced by the inclusion of LiCl in the reaction of MeCuI·MgCl.

proposed that similar reaction mechanisms are involved in S_N2 reactions of organocuprates.[27]

It is tempting to envisage the reaction mechanism of lithium-induced *anti*-S_N2' selectivity, as shown in Figure 4. According to this model, MeCuI·MgCl is initially converted to the cluster **41** by the addition of lithium chloride. The formation of the cluster **41** may be adequate because **41** has been identified as

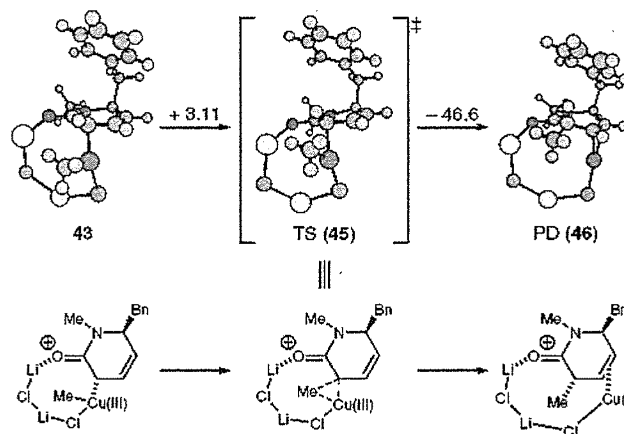

FIGURE 5. Optimized geometries of complex **43**, TS (**45**) and PD (**46**) in the gas phase at the B3LYP/631A level. The energy changes in kcal/mol are given above the arrows.

a reaction product in a theoretical study on the S_N2 reaction of organocuprates by Nakamura et al.[27] The cluster **41** approaches the phosphate **24** while coordinating the carbonyl oxygen with a lithium atom to form complex **42**. The resulting complex **42** is then preferentially converted to the Cu(III) complex **43** with an *anti*-S_N2' interaction of the intramolecular organocopper moiety. Rapid reductive elimination of **43** results predominantly in the formation of the *anti*-S_N2' product **25**. It is hypothesized that magnesium salts cannot induce the formation of the cluster structure such as **41** for electrostatic and structural reasons. Therefore, both the α- and γ-carbons would be attacked by "MeCu" without coordination between the organocopper species and the carbonyl oxygen, leading to a mixture of *anti*-S_N2' and S_N2 products (Figure 4, **44**). The reactivity of CN-containing organocopper cluster reagents may differ from that of cluster **41**. Decreased regioselectivity induced by $BF_3 \cdot Et_2O$ may result from decomposition of the organocopper cluster or disruption of interactions between the organocopper species and the carbonyl oxygen.

We performed density functional theory (DFT)[28] calculations on the basis of the plausible route from **43** to **25** (Figure 5). As shown in Figure 5, these calculations confirm that reductive elimination of complex **43** proceeds smoothly via transition state **45** with a reasonable activation energy (3.11 kcal/mol) to yield complex **46**, which leads to the *anti*-S_N2' product **25**. These results support the above explanation for the improvement of *anti*-S_N2' selectivity induced by LiCl.

Next, organocopper-mediated *anti*-S_N2' reactions of *N*-DMB-phosphate derivative **47** were carried out. (Scheme 6). All reactions proceeded smoothly to afford the *anti*-S_N2' products **48–50**.[29] After removal of the DMB group under acidic conditions, the resulting lactams were converted into the corresponding (*Z*)-alkene dipeptide isosteres using Guibé's methodology.[5a] These represent *cis*-peptide bond equivalents,[11] indicating that our novel synthetic methodology for the preparation of DKP mimetics may also afford a potential strategy for the stereoselective synthesis of (*Z*)-alkene dipeptide isosteres.

Encouraged by this methodology for the stereoselective preparation of diketopiperazine mimetics, we conducted the

(25) (a) Snyder, J. P.; Spangler, D. P.; Behling, J. R.; Rossiter, B. E. *J. Org. Chem.* **1994**, *59*, 2665. (b) Snyder, J. P.; Bertz, S. H. *J. Org. Chem.* **1995**, *60*, 4312. (c) Bertz, S. H.; Vellekoop, A. S.; Smith, R. A. J.; Snyder, J. P. *Organometallics* **1995**, *14*, 1213. (d) Gerold, A.; Jastrzebski, J. T. B. H.; Kronenburg, C. M. P.; Krause, N.; van Koten, G. *Angew. Chem., Int. Ed. Engl.* **1997**, *36*, 755. (e) Bertz, S. H.; Chopra, A.; Eriksson, M.; Ogle, C. A.; Seagle, P. *Chem.—Eur. J.* **1999**, *5*, 2680. (f) Gschwind, R. M.; Rajamohanan, P. R.; John, M.; Boche, G. *Organometallics* **2000**, *19*, 2868. (g) Gschwind, R. M.; Xie, X.; Rajamohanan, P. R.; Auel, C.; Boche, G. *J. Am. Chem. Soc.* **2001**, *123*, 7299. (h) Canisius, J.; Mobley, T. A.; Berger, S.; Krause, K. *Chem.—Eur. J.* **2001**, *7*, 2671. (i) Mori, S.; Nakamura, E.; Morokuma, K. *Organometallics* **2004**, *23*, 1081. (j) Mori, S.; Uerdingen, M.; Krause, N.; Morokuma, K. *Angew. Chem., Int. Ed.* **2005**, *44*, 4715. (k) Yoshikai, N.; Yamashita, T.; Nakamura, E. *Angew. Chem., Int. Ed.* **2005**, *44*, 4721. (l) Henze, W.; Vyater, A.; Krause, N.; Gschwind, R. M. *J. Am. Chem. Soc.* **2005**, *127*, 17335.

(26) (a) Nakamura, E.; Mori, S.; Nakamura, M.; Morokuma, K. *J. Am. Chem. Soc.* **1997**, *119*, 4887. (b) Nakamura, E.; Mori, S.; Morokuma, K. *J. Am. Chem. Soc.* **1997**, *119*, 4900. (c) Nakamura, E.; Mori, S. *Angew. Chem., Int. Ed.* **2000**, *39*, 3750. (d) Yamanaka, M.; Nakamura, E. *Organometallics* **2001**, *20*, 5675. (e) Nakamura, E.; Yoshikai, N. *Bull. Chem. Soc. Jpn.* **2004**, *77*, 1.

(27) Nakamura, E.; Mori, S.; Morokuma, K. *J. Am. Chem. Soc.* **1998**, *120*, 8273.

(28) (a) Seminario, J. M., Politzer, P., Eds. *Modern Density Functional Theory. A Tool for Chemistry*; Elsevier: New York, 1995; Vol. 2 (Theoretical and Computational Chemistry). (b) Koch, W.; Holthausen, M. C. *A Chemist's Guide to Density Functional Theory*; Wiley-VCH: Weinheim, Germany, 2000.

SCHEME 6. Organocopper-Mediated *anti*-S_N2' Reaction of *N*-DMB Derivative 47[a]

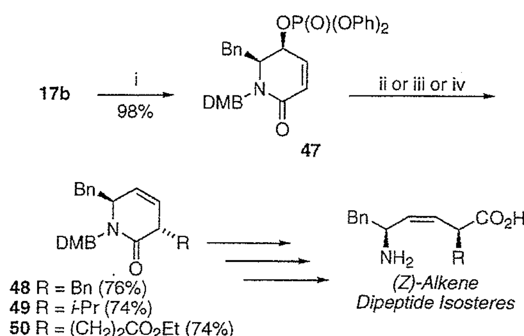

[a] Reagents and conditions: (i) $(PhO)_2P(O)Cl$, pyridine, CH_2Cl_2; (ii) $BnCuI{\cdot}MgCl{\cdot}2LiCl$, THF, −78 °C, 20 min; (iii) i-$PrCu(CN){\cdot}MgCl{\cdot}2LiCl$, THF, −78 °C, 20 min; (iv) $BrZnCu(CN){\cdot}CH_2CH_2CO_2Et$, THF, 0 °C, 60 min.

synthesis of a biologically relevant DKP mimetic designed as a CXCR4-chemokine receptor antagonist (Scheme 7). CXCR4 is a seven-transmembrane G-protein-coupled receptor, which is involved in HIV infection, cancer metastasis, and other disease processes.[30] Thus, CXCR4 is thought to be an attractive therapeutic target for these problematic diseases.[31] Recently, we identified a cyclic pentapeptide, *cyclo*-(-Nal-Gly-D-Tyr-Arg-Arg-), possessing strong CXCR4 antagonistic activity.[32] In this peptide, guanidyl and naphthyl side chains proved to be especially important pharmacophores for the antagonistic activity. We hypothesized that DKP mimetics having guanidine and naphthalene moieties such as **62** could exhibit CXCR4 antagonistic activity. The synthesis of **62** started from L-2-naphthylalanine **51**, which was converted to *N*-Boc-protected methyl ester **52** (esterification with $SOCl_2$ and MeOH, followed by *N*-protection). After reduction of the ester **52**, the resulting aldehyde was treated with vinyl Grignard reagent in the presence of zinc and lithium salts to yield the *syn*-allylic alcohol **53** along with a small amount of the anti isomer. Following Boc deprotection of **53**, *O*-TBS protected Ns-amide **54** was synthesized by a procedure identical to that used to prepare **12**. *N*-Alkylation of **54** with $BocNHCH_2(CH_2)_2CH_2I$[33] yielded amide **55**, which was converted to phosphate **58** by a sequence of reactions, including ring-closing metathesis. The reaction of phosphate **58** with $TBSOCH_2(CH_2)_2CH_2Cu(CN)Li{\cdot}LiI{\cdot}2LiCl$ proceeded smoothly in an *anti*-S_N2' manner[34] to afford the alkylated product **59** as the sole product. After removal of the TBS group with H_2SiF_6, the resulting alcohol **60** was subjected to guanidylation with 1,3-bis(*tert*-butoxycarbonyl)guanidine under Mitsunobu conditions[35] to afford compound **61**. *N*-Boc deprotection of **61** followed by guanidylation[8d] of the resulting amine and HPLC purification yielded the desired DKP mimetic **62**, which showed significant CXCR4 antagonistic activity (IC_{50} = 15.1 μM). Although the antagonistic activity of mimetic **62** has yet to reach the level for clinical usage, the 3,6-dihydropyridin-2-one could be a potential scaffold for the development of novel low molecular weight CXCR4 antagonists.

Conclusion

In conclusion, regio- and stereoselective alkylations of γ-phosphoryloxy-α,β-unsaturated-δ-lactams with organocopper reagents were carefully examined for the synthesis of highly functionalized DKP mimetics. Organocopper reagents, which were prepared from equimolar amounts of an organometallic (Li, Mg or Zn) reagent and a copper salt in the presence of LiCl, proved to be suitable for these transformations. This reaction system features several advantages for the diversity-oriented synthesis of DKP mimetics in terms of available organocopper reagents, stereoselectivity, and tolerance of functional groups. Dramatic improvement of regioselectivity induced by LiCl in the reaction of $MeCuI{\cdot}MgCl$ can be rationalized by a "trap and bite" mechanism in which organocopper cluster structures containing LiCl are responsible for determining regioselectivity. Such a hypothesis was supported by a DFT calculation. Finally, compound **62**, a potential lead for the development of low molecule CXCR4 antagonists was synthesized by a reaction sequence utilizing an organocopper-mediated *anti*-S_N2' reaction of phosphate **58**. Details of the reaction mechanisms involving organocopper cluster formation are currently being investigated.

Experimental Section

(3*S*,4*S*)-3-[(*tert*-Butyl)dimethylsiloxy]-4-[*N*-methyl-*N*-(2-nitrobenzenesulfonyl)amino]-5-phenylpent-1-en (12a). To a stirred solution of sulfonamide *syn*-**11** (500 mg, 1.05 mmol) in DMF (5

SCHEME 7. Synthesis of a Biologically Relevant DKP Mimetic 62 Designed as a CXCR4-Chemokine Receptor Antagonist[a]

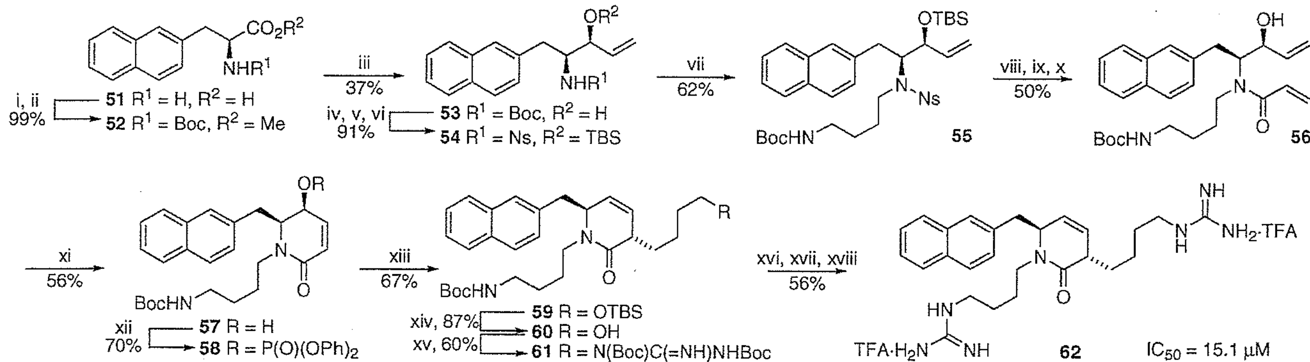

[a] Reagents and conditions: (i) $SOCl_2$, MeOH; (ii) Boc_2O, $(i\text{-}Pr)_2NEt$, $CHCl_3$; (iii) DIBAL-H, CH_2Cl_2−toluene then $CH_2{=}CHMgCl$, $ZnCl_2$, LiCl, THF; (iv) 4 M HCl−dioxane; (v) Ns-Cl, 2,4,6-collidine, $CHCl_3$; (vi) TBSOTf, 2,6-lutidine, CH_2Cl_2; (vii) $BocNHCH_2(CH_2)_2CH_2I$, K_2CO_3, DMF; (viii) $HSCH_2CO_2H$, $LiOH{\cdot}H_2O$, DMF; (ix) $CH_2{=}CHCOCl$, Et_3N, CH_2Cl_2; (x) TBAF, THF; (xi) Grubbs' cat. second generation, CH_2Cl_2; (xii) $(PhO)_2P(O)Cl$, pyridine, CH_2Cl_2; (xiii) $TBSOCH_2(CH_2)_2CH_2Cu(CN)Li{\cdot}LiI{\cdot}2LiCl$, *n*-pentane-THF; (xiv) H_2SiF_6, CH_3CN; (xv) 1,3-bis(*tert*-butoxycarbonyl)guanidine, PPh_3, diisopropyl azodicarboxylate, THF; (xvi) 95% aq CF_3CO_2H; (xvii) 1*H*-pyrazole-1-carboxamidine hydrochloride, $(i\text{-}Pr)_2NEt$, DMF; (xviii) RP-HPLC purification. Abbreviation: TFA, trifluoroacetic acid.

mL) were added K_2CO_3 (724 mg, 5.24 mmol) and MeI at 0 °C. After stirring the mixture for 1 h at room temperature, the whole was extracted with EtOAc. The extract was washed with brine and dried over $MgSO_4$. Concentration under reduced pressure followed by flash chromatography over silica gel with *n*-hexanes−EtOAc (6:1) gave the title compound **12a** (507 mg, 98.6%) as colorless crystals: mp 74−75 °C; $[\alpha]^{33}_D$ −49.8 (*c* 1.02, $CHCl_3$); ^1H NMR (270 MHz, $CDCl_3$) δ 0.03 (s, 3H), 0.08 (s, 3H), 0.95 (s, 9H), 2.80 (dd, *J* = 14.1, 8.7 Hz, 1H), 3.08 (s, 3H), 3.11 (dd, *J* = 13.8, 6.2 Hz, 1H), 4.12−4.24 (m, 1H), 4.32−4.24 (m, 1H), 5.08 (d, *J* = 10.5 Hz, 1H), 5.19 (dt, *J* = 17.1, 1.3 Hz, 1H), 5.90 (ddd, *J* = 17.1, 10.2, 6.9 Hz, 1H), 7.07−7.18 (m, 5H), 7.25−7.55 (m, 4H); ^{13}C NMR (100 MHz, $CDCl_3$) δ −4.8, −3.7, 18.3, 26.1, 31.6, 33.9, 64.1, 75.9, 117.1, 123.6, 126.4, 128.3, 128.9, 130.3, 131.1, 132.5, 133.0, 137.9, 147.8. Anal. Calcd for $C_{24}H_{34}N_2O_5SSi$: C, 58.75; H, 6.98; N, 5.71. Found: C, 58.71; H, 7.05; N, 5.69.

(3*S*,4*S*)-4-(*N*-Acryloyl-*N*-methylamino)-3-[(*tert*-butyl)dimethylsiloxy]-5-phenylpent-1-en (13a). To a stirred solution of the *N*-Me-sulfonamide **12a** (507 mg, 1.03 mmol) in DMF (3.6 mL) were added LiOH·H_2O (260 mg, 6.20 mmol) and $HSCH_2CO_2H$ (216 μL, 1.26 mmol) at 0 °C, and the mixture was stirred for 2 h at room temperature. The mixture was extracted with EtOAc. The extract was washed with saturated $NaHCO_3$ and dried over $MgSO_4$. Concentration under reduced pressure gave oily residues that were dissolved in CH_2Cl_2 (5 mL). Et_3N (720 μL, 5.17 mmol) and acryloyl chloride (336 μL, 1.01 mmol) were added dropwise to the above solution at −20 °C, and the mixture was stirred for 1.5 h at 0 °C under argon. Saturated $NaHCO_3$ (2 mL) was added to the above mixture at 0 °C, and the whole was extracted with EtOAc. The extract was washed successively with saturated citric acid, brine, saturated $NaHCO_3$, and brine and dried over $MgSO_4$. Concentration under reduced pressure followed by flash chromatography over silica gel with *n*-hexanes−EtOAc (6:1) gave the title compound **13a** (316 mg, 83.8% yield) as a colorless oil (rotamer mixture): $[\alpha]^{33}_D$ −51.3 (*c* 0.94, $CHCl_3$); ^1H NMR (600 MHz at 323 K, $CDCl_3$) δ 0.04 (s, 6H), 0.06 (s, 3H), 0.07 (s, 3H), 0.88 (s, 9H), 0.92 (9H), 2.81 (dd, *J* = 14.3, 10.6 Hz, 1H), 2.84−2.90 (m, 1H), 2.87 (s, 3H), 2.91−2.97 (m, 1H), 2.94 (s, 3H), 3.02−3.08 (m, 1H), 4.02 (ddd, *J* = 10.4, 6.2, 4.1 Hz, 1H), 4.20 (t, *J* = 6.8 Hz, 1H), 4.40−4.50 (m, 1H), 4.65−4.80 (m, 1H), 5.15 (d, *J* = 10.4 Hz, 1H), 5.24−5.30 (m, 3H), 5.33 (dd, *J* = 10.8, 1.8 Hz, 1H), 5.52 (dd, *J* = 10.5, 2.0 Hz, 1H), 5.75−5.90 (m, 3H), 6.10 (dd, *J* = 16.8, 2.0 Hz, 1H), 6.18 (dd, *J* = 17.0, 10.8 Hz, 1H), 6.36 (dd, *J* = 16.8, 10.5 Hz, 1H), 7.05−7.26 (m, 10H); ^{13}C NMR (100 MHz, $CDCl_3$) δ −5.0, −4.9, −4.1, −3.9, 17.9, 18.0, 25.5, 25.6, 25.8, 28.3, 34.1, 34.8, 63.5, 73.6, 75.0, 75.4, 115.6, 117.4, 125.2, 125.8, 126.1, 126.2, 126.7, 127.9, 128.2, 128.4, 128.6, 129.0, 137.4, 138.0, 138.2, 138.4, 166.6, 168.2; HRMS (FAB) *m*/*z* calcd for $C_{21}H_{34}NO_2Si$ (MH^+), 360.2359; found, 360.2352.

(3*S*,4*S*)-4-(*N*-Acryloyl-*N*-methylamino)-5-phenylpent-1-en-3-ol (16a). The acrylamide **13a** (116 mg, 0.322 mmol) was dissolved in 1.0 M TBAF in THF (1 mL) at 0 °C, and the mixture was stirred for 3 h at room temperature. The mixture was extracted with EtOAc. The extract was washed with brine and dried over $MgSO_4$. Concentration under reduced pressure followed by flash chromatography over silica gel with *n*-hexanes−EtOAc (3:1) gave the title compound **16a** (78.2 mg, 98.9% yield) as a colorless oil (rotamer mixture): $[\alpha]^{29}_D$ −92.2 (*c* 1.58, $CHCl_3$); ^1H NMR (600 MHz, $CDCl_3$) δ 2.75 (s, 3H), 2.78 (dd, *J* = 14.4, 10.5 Hz, 0.3H), 2.94 (dd, *J* = 14.2, 4.1 Hz, 0.3H), 2.97 (s, 0.9H), 3.06 (dd, *J* = 14.0, 5.5 Hz, 1H), 3.10−3.30 (m, 1H), 4.01 (ddd, *J* = 10.9, 7.4, 4.2 Hz, 0.3H), 4.22 (t, *J* = 7.2 Hz, 0.3H), 4.26 (m, 1H), 5.16 (d, *J* = 10.5 Hz, 1H), 5.31 (d, *J* = 10.3 Hz, 0.3H), 5.37 (dt, *J* = 17.1, 1.4 Hz, 1H), 5.35−5.45 (m, 0.6H), 5.66 (dd, *J* = 10.4, 1.7 Hz, 1H), 5.80−5.90 (m, 1.6H), 6.16 (dd, *J* = 16.9, 10.8 Hz, 0.3H), 6.24 (dd, *J* = 16.7, 1.3 Hz, 1H), 6.38 (dd, *J* = 16.8, 10.4 Hz, 1H), 7.00−7.30 (m, 6.5H); ^{13}C NMR (100 MHz, $CDCl_3$) δ 28.1, 34.4, 34.9, 63.5, 73.5, 73.8, 115.6, 118.4, 126.0, 126.2, 126.5, 128.1, 128.2, 128.3, 128.4, 128.6, 128.7, 128.8, 137.3, 138.4, 168.0, 168.6; HRMS (FAB) *m*/*z* calcd for $C_{15}H_{20}NO_2$ (MH^+), 246.1494; found, 246.1490.

(5*S*,6*S*)-6-Benzyl-5,6-dihydro-5-hydroxy-1-methylpyridin-2-one (17a). To a solution of the acrylamide **16a** (750 mg, 3.05 mmol) in CH_2Cl_2 (20 mL) was added Grubbs' catalyst second generation (129 mg, 0.152 mmol), and the mixture was stirred for 6 h at room temperature under argon. Concentration under reduced pressure followed by flash chromatography over silica gel with *n*-hexanes−EtOAc (1:1) gave the title compound **17a** (558 mg, 84.2% yield) as colorless crystals: mp 96−97 °C; $[\alpha]^{28}_D$ −137.1 (*c* 1.06, $CHCl_3$); ^1H NMR (270 MHz, $CDCl_3$) δ 2.56 (s, 3H), 2.97 (dd, *J* = 13.5, 9.2 Hz, 1H), 3.19 (dd, *J* = 13.5, 4.6 Hz, 1H), 3.60−3.85 (m, 2H), 4.87 (m, 1H), 5.85 (d, *J* = 9.8 Hz, 1H), 6.42 (d, *J* = 9.8 Hz, 1H), 7.14−7.35 (m, 5H); ^{13}C NMR (100 MHz, $CDCl_3$) δ 33.1, 35.1, 65.6, 66.7, 122.8, 126.2, 128.3, 129.2, 138.3, 143.7, 163.6. Anal. Calcd for $C_{13}H_{15}NO_2$: C, 71.87; H, 6.96; N, 6.45. Found: C, 71.69; H, 7.01; N, 6.37.

(5*S*,6*S*)-6-Benzyl-5,6-dihydro-5-diphenylphosphoryloxy-1-methylpyridine-2-one (24). To a solution of the alcohol **17a** (450 mg, 2.07 mmol) and pyridine (1.33 mL, 16.5 mmol) in CH_2Cl_2 (7.5 mL) was added dropwise diphenylphosphoryl chloride (1.72 mL, 8.28 mmol) at 0 °C, and the mixture was stirred at 0 °C for 4 h. H_2O (10 mL) was added to the above mixture, and the whole was extracted with EtOAc. The extract was washed successively with saturated citric acid, brine, saturated $NaHCO_3$, and brine and dried

(29) Relative configurations of **48** and **49** were assigned as 3,6-trans derivatives based on the published data (ref 5). The observed chemical shifts of the α-protons of **48** and **49** (2.45 and 2.16 ppm, respectively) were nearly identical to those of the corresponding *N*-methyl derivatives **27** and **28** (2.41 and 2.14 ppm, respectively). We also confirmed that the α-proton of the corresponding 3,6-cis diastereomer of **48** appeared downfield (3.16 ppm) in comparison with **48**, as in the cases of *N*-methyl derivatives. The α-proton chemical shift of **50** was 2.29 ppm, which is similar to that of the corresponding *N*-methyl-3,6-trans derivative **30** (2.21 ppm). Based on these data, compound **50** was assigned as 3,6-trans.

(30) (a) Feng, Y.; Broder, C. C.; Kennedy, P. E.; Berger, E. A. *Science* **1996**, *272*, 872. (b) Koshiba, T.; Hosotani, R.; Miyamoto, Y.; Ida, J.; Tsuji, S.; Nakajima, S.; Kawaguchi, M.; Kobayashi, H.; Doi, R.; Hori, T.; Fujii, N.; Imamura, M. *Clin. Cancer Res.* **2000**, *6*, 3530. (c) Nanki, T.; Hayashida, K.; El-Gabalawy, H. S.; Suson, S.; Shi, K.; Girshick, H. J.; Yavuz, S.; Lipsky, P. E. *J. Immunol.* **2000**, *165*, 6590. (d) Müller, A.; Homey, B.; Soto, H.; Ge, N.; Catron, D.; Buchanan, M. E.; McClanahan, T.; Murphy, E.; Yuan, W.; Wagner, S. N.; Barrera, J. L.; Mohar, A.; Verastegui, E.; Zlotnik, A. *Nature* **2001**, *410*, 50. (e) Tamamura, H.; Hori, A.; Kanzaki, N.; Hiramatsu, K.; Mizumoto, M.; Nakashima, H.; Yamamoto, N.; Otaka, A.; Fujii, N. *FEBS Lett.* **2003**, *550*, 79. (f) Tamamura, H.; Fujisawa, M.; Hiramatsu, K.; Mizumoto, M.; Nakashima, H.; Yamamoto, N.; Otaka, A.; Fujii, N. *FEBS Lett.* **2004**, *569*, 99.

(31) For an example of CXCR4 inhibitors, see: (a) Schols, D.; Struyf, S.; Van Damme, J.; Este, J. A.; Henson, G.; De Clercq, E. *J. Exp. Med.* **1997**, *186*, 1383. (b) Murakami, T.; Nakajima, T.; Koyanagi, Y.; Tachibana, K.; Fujii, N.; Tamamura, H.; Yoshida, N.; Waki, M.; Matsumoto, A.; Yoshie, O.; Kishimoto, T.; Yamamoto, N.; Nagasawa, T. *J. Exp. Med.* **1997**, *186*, 1389. (c) Doranz, B. J.; Grovit-Ferbas, K.; Sharron, M. P.; Mao, S.-H.; Bidwell Goetz, M.; Daar, E. S.; Doms, R. W.; O'Brien, W. A. *J. Exp. Med.* **1997**, *186*, 1395. (d) Donzella, G. A.; Schols, D.; Lin, S. W.; Este, J. A.; Nagashima, K. A.; Maddon, P. J.; Allaway, G. P.; Sakmar, T. P.; Henson, G.; De Clercq, E.; Moore, J. P. *Nat. Med.* **1998**, *4*, 72. (e) Howard, O. M. Z.; Oppenheim, J. J.; Hollingshead, M. G.; Covey, J. M.; Bigelow, J.; McCormack, J. J.; Buckheit, R. W., Jr.; Clanton, D. J.; Turpin, J. A.; Rice, W. G. *J. Med. Chem.* **1998**, *41*, 2184.

(32) Fujii, N.; Oishi, S.; Hiramatsu, K.; Araki, T.; Ueda, S.; Tamamura, H.; Otaka, A.; Kusano, S.; Terakubo, S.; Nakashima, H.; Broach, J. A.; Trent, J. O.; Wang, Z.; Peiper, S. C. *Angew. Chem., Int. Ed.* **2003**, *42*, 3251.

(33) Lamothe, S.; Zacharie, B.; Attardo, G.; Labrecque, D.; Courchesne, M.; Falardeau, G.; Rej, R.; Abbott, S. PCT Int. Appl. WO 2000017197 A1 20000330, 2000; p 187.

(34) In ^1H NMR experiments, the α-proton of compound **59** was detected at higher field (2.20 ppm) in comparison with that of the corresponding diastereomer (2.72 ppm). This can be rationalized by the anisotropic effect of the naphthalene ring, as in the case of phenylalanine-derived compounds. Based on these data, the relative configuration of **59** was assigned as 3,6-trans. See the Supporting Information.

(35) (a) Dodd, D. S.; Kozikowski, A. P. *Tetrahedron Lett.* **1994**, *35*, 977. (b) Beumer, R.; Reiser, O. *Tetrahedron* **2001**, *57*, 6497.

over $MgSO_4$. Concentration under reduced pressure followed by flash chromatography over silica gel with *n*-hexanes−EtOAc (1:1) gave the title compound **24** (790 mg, 84.8% yield) as a colorless oil: $[\alpha]^{26}_D$ −25.8 (*c* 0.28, $CHCl_3$); ^1H NMR (400 MHz, $CDCl_3$) δ 2.46 (s, 3H), 2.92 (dd, *J* = 13.6, 7.2 Hz, 1H), 3.00 (dd, *J* = 13.6, 3.0 Hz, 1H), 3.83 (m, 1H), 5.69 (m, 1H), 5.88 (dd, *J* = 10.0, 0.8 Hz, 1H), 6.29 (dt, *J* = 10.0, 1.6 Hz, 1H), 7.00−7.07 (m, 2H), 7.17−7.44 (m, 13H); ^{13}C NMR (100 MHz, $CDCl_3$) δ 33.3, 34.8, 63.2, 63.3, 73.5, 73.6, 119.5, 119.6, 119.7, 125.0, 125.4, 126.3, 128.2, 129.0, 129.5, 136.8, 137.0, 137.1, 149.7, 149.8, 161.9; HRMS (FAB) *m/z* calcd for $C_{25}H_{25}NO_5P$ (MH^+), 450.1470; found, 450.1462.

General Procedure for the Organocopper-Mediated *anti*-S_N2' Reaction of γ-Phosphoryloxy-α,β-unsaturated-δ-lactams. Synthesis of (3*S*,6*S*)-6-Benzyl-3,6-dihydro-1,3-dimethylpyridin-2-one (25). To a solution of CuI (37.3 mg, 0.196 mmol) and anhydrous LiCl (16.6 mg) in THF (0.75 mL) was added dropwise a solution of MeMgCl in THF (3.0 M, 65.3 μL, 0.196 mmol) at −78 °C under argon, and the mixture was stirred for 10 min at 0 °C. To the above mixture, was added dropwise a solution of the lactam **24** (44.1 mg, 0.0981 mmol) in THF (0.75 mL) at −78 °C, and the mixture was stirred for 20 min at −78 °C. The reaction was quenched at −78 °C by the addition of a 1:1 saturated NH_4Cl/28% NH_4OH solution (2 mL), with additional stirring at room temperature for 30 min. The mixture was extracted with Et_2O, and the extract was washed with H_2O and dried over $MgSO_4$. Concentration under reduced pressure followed by flash chromatography over silica gel with *n*-hexanes−EtOAc (1:1) gave the title compound **25** (19.6 mg, 92.8% yield) as a colorless oil: $[\alpha]^{23}_D$ +231.9 (*c* 0.21, $CHCl_3$); ^1H NMR (600 MHz, $CDCl_3$) δ 1.16 (d, *J* = 7.5 Hz, 3H), 2.11−2.17 (m, 1H), 2.88 (dd, *J* = 13.4, 3.7 Hz, 1H), 2.93 (dd, *J* = 13.5, 6.6 Hz, 1H), 3.08 (s, 3H), 4.08−4.14 (m, 1H); 5.55 (dd, *J* = 10.1, 2.1 Hz, 1H), 5.62 (ddd, *J* = 9.9, 4.3, 2.9 Hz, 1H), 7.05−7.32 (m, 5H); ^{13}C NMR (100 MHz, $CDCl_3$) δ 17.7, 33.1, 34.9, 39.3, 61.6, 123.5, 126.3, 127.8, 129.5, 129.9, 135.5, 171.4; HRMS (FAB) *m/z* calcd for $C_{14}H_{18}NO$ (MH^+), 216.1388; found, 216.1389.

(5*R*,6*S*)-6-Benzyl-5,6-dihydro-1,5-dimethylpyridin-2-one (S_N2-25). A colorless oil: $[\alpha]^{24}_D$ −212.0 (*c* 0.49, $CHCl_3$); ^1H NMR (400 MHz, $CDCl_3$) δ 1.05 (d, *J* = 7.1 Hz, 3H), 2.31 (m, 1H), 2.73 (dd, *J* = 13.4, 9.0 Hz, 1H), 2.91 (s, 3H), 3.00 (dd, *J* = 13.4, 5.8 Hz, 1H), 3.31 (m, 1H), 5.93 (d, *J* = 9.8 Hz, 1H), 6.45 (ddd, *J* = 9.8, 6.1, 1.7 Hz, 1H), 7.07−7.40 (m, 5H); ^{13}C NMR (100 MHz, $CDCl_3$) δ 18.8, 31.5, 34.5, 38.3, 66.6, 123.6, 126.7, 128.7, 129.2, 137.8, 142.7, 163.2; HRMS (FAB) *m/z* calcd for $C_{14}H_{18}NO$ (MH^+), 216.1388; found, 216.1393.

(3*S*,6*S*)-1-{4-[(*tert*-Butoxycarbonyl)amino]butyl}-3-{4-[(*tert*-butyl)dimethylsiloxy]butyl}-3,6-dihydro-6-[(2-naphthyl)methyl]-pyridin-2-one (59). By use of a procedure identical with that described for the preparation of **29** from **24**, treatment of the phosphate **58** (196 mg, 0.300 mmol) with $TBSOCH_2(CH_2)_2CH_2$-Cu(CN)Li·LiI·2LiCl (4 equiv) at −78 °C for 1 h gave the title compound **59** (120 mg, 67.2% yield) as a colorless oil: $[\alpha]^{23}_D$ +80.3 (*c* 1.06, $CHCl_3$); ^1H NMR (400 MHz, $CDCl_3$) δ 0.00 (s, 6H), 0.85 (s, 9H), 1.11−1.23 (m, 2H), 1.43 (s, 9H), 1.38−1.72 (m, 8H), 2.14−2.25 (m, 1H), 2.93−3.23 (m, 5H), 3.45−3.59 (m, 2H), 4.04−4.27 (m, 2H), 4.64−4.76 (m, 1H), 5.58 (dd, *J* = 10.0, 2.0 Hz, 1H), 5.64−5.75 (m, 1H), 7.17−7.30 (m, 1H), 7.40−7.60 (m, 3H), 7.70−7.86 (m, 3H); ^{13}C NMR (100 MHz, $CDCl_3$) δ −5.3, 18.3, 22.0, 24.7, 25.9, 27.5, 28.4, 31.1, 32.7, 39.9, 40.0, 40.3, 44.4, 59.0, 62.9, 79.0, 125.1, 125.6, 126.0, 127.5, 127.6, 127.7, 127.9, 128.3, 128.5, 132.1, 133.2, 133.7, 156.0, 170.7; HRMS (FAB) *m/z* calcd for $C_{35}H_{55}N_2O_4Si$ (MH^+), 595.3931; found, 595.3939.

(3*S*,6*S*)-1-{4-[(*tert*-Butoxycarbonyl)amino]butyl}-3,6-dihydro-3-(4-hydroxy)butyl-6-[(2-naphthyl)methyl]pyridin-2-one (60). To a solution of the lactam **59** (102 mg, 0.172 mmol) in CH_3CN (1.7 mL) was added a solution of H_2SiF_6 in H_2O (3.23 M, 11.0 μL, 0.0357 mmol) at 0 °C, and the mixture was stirred for 1 h at 0 °C. Saturated aq K_2CO_3 (2 mL) was added to the above mixture, and the whole was extracted with Et_2O. The extract was washed successively with saturated K_2CO_3 and brine and dried over $MgSO_4$. Concentration under reduced pressure followed by flash chromatography over silica gel with *n*-hexanes−EtOAc (1:3) gave the title compound **60** (69.8 mg, 87.2% yield) as a colorless oil: $[\alpha]^{24}_D$ +142.3 (*c* 1.14, $CHCl_3$); ^1H NMR (400 MHz, $CDCl_3$) δ 1.12−1.35 (m, 4H), 1.43 (s, 9H), 1.39−1.56 (m, 4H), 1.58−1.73 (m, 2H), 1.73−1.88 (m, 1H), 2.15−2.25 (m, 1H), 2.95−3.11 (m, 3H), 3.08−3.22 (m, 2H), 3.50−3.65 (m, 2H), 4.10−4.28 (m, 2H), 4.80−4.94 (m, 1H), 5.57 (dd, *J* = 10.0, 2.0 Hz, 1H), 5.63−5.78 (m, 1H), 7.18−7.30 (m, 1H), 7.40−7.60 (m, 3H), 7.70−7.85 (m, 3H); ^{13}C NMR (100 MHz, $CDCl_3$) δ 21.7, 24.7, 27.5, 28.4, 30.5, 32.2, 39.9, 40.0, 40.1, 44.3, 59.0, 62.2, 79.0, 125.2, 125.6, 126.0, 127.5, 127.6, 127.7, 127.9, 128.5, 128.6, 132.1, 133.2, 133.6, 156.1, 171.0; HRMS (FAB) *m/z* calcd for $C_{29}H_{41}N_2O_4$ (MH^+), 481.3066; found, 481.3060.

(3*S*,6*S*)-3-{4-{[*N*,*N*-Bis(*tert*-butoxycarbonyl)guanidino]}butyl}-1-{4-[(*tert*-butoxycarbonyl)amino]butyl}-3,6-dihydro-6-[(2-naphthyl)methyl]pyridin-2-one (61). To a solution of the alcohol **60** (62.6 mg, 0.183 mmol), PPh_3 (144 mg, 0.548 mmol), and 1,3-bis-(*tert*-butoxycarbonyl)guanidine (142 mg, 0.548 mmol) in THF (0.98 mL) was added dropwise a solution of diisopropyl azodicarboxylate in toluene (1.9 M, 288 mL, 0.548 mmol) at 0 °C under argon, and the mixture was stirred for 12 h at room temperature. Concentration under reduced pressure followed by flash chromatography over silica gel with *n*-hexanes−EtOAc (3:1) gave the title compound **61** (66.8 mg, 50.7% yield) as a colorless oil: $[\alpha]^{24}_D$ +103.3 (*c* 0.79, $CHCl_3$); ^1H NMR (400 MHz, $CDCl_3$) δ 1.07−1.69 (m, 37H), 2.17−2.25 (m, 1H), 2.94−3.26 (m, 5H), 3.67−3.95 (m, 2H), 4.13 (m, 1H), 4.17−4.27 (m, 1H), 4.74−4.89 (m, 1H), 5.58 (dd, *J* = 10.0, 1.6 Hz, 1H), 5.66−5.77 (m, 1H), 7.17−7.28 (m, 1H), 7.38−7.60 (m, 3H), 7.69−7.86 (m, 3H); ^{13}C NMR (100 MHz, $CDCl_3$) δ 22.9, 24.8, 27.6, 28.0, 28.3, 28.4, 28.7, 31.0, 39.9, 40.1, 40.2, 44.3, 44.4, 59.0, 83.5, 125.1, 125.6, 126.0, 127.5, 127.7, 127.9, 128.3, 128.6, 132.1, 133.2, 133.6, 155.1, 156.0, 160.6, 163.8, 170.6; HRMS (FAB) *m/z* calcd for $C_{40}H_{60}N_5O_7$ (MH^+), 722.4493; found, 722.4482.

(3*S*,6*S*)-1,3-Bis(4-guanidinobutyl)-3,6-dihydro-6-[(2-naphthyl)-methyl]pyridin-2-one Trifluoroacetate (62). The lactam **61** (47.8 mg, 0.0662 mmol) was dissolved in 95% aq TFA (1.2 mL), and the mixture was stirred for 4 h at room temperature. Concentration under reduced pressure gave an oily residue, which was dissolved in DMF (0.1 mL). 1*H*-pyrazole-1-carboxamidine hydrochloride (29.1 mg, 0.198 mmol) and $(i\text{-}Pr)_2NEt$ (210 μL, 1.23 mmol) was added to the above mixture at 0 °C, and the mixture was stirred overnight at room temperature. Concentration under reduced pressure and purification by preparative HPLC gave the title compound **62** (15.4 mg, 33.6% yield) as a freeze-dried powder: $[\alpha]^{21}_D$ +132.5 (*c* 0.35, CH_3OH); ^1H NMR (400 MHz, CD_3OD) δ 1.04−1.19 (m, 2H), 1.30−1.40 (m, 2H), 1.54−1.74 (m, 5H), 2.96−3.08 (m, 3H), 3.14−3.30 (m, 4H), 4.02−4.15 (m, 1H), 4.36−4.45 (m, 1H), 5.59 (dd, *J* = 9.8, 2.0 Hz, 1H), 5.87−5.96 (m, 1H), 7.21−7.28 (m, 1H), 7.37−7.49 (m, 2H), 7.56 (s, 1H), 7.70−7.84 (m, 3H); ^{13}C NMR (100 MHz, CD_3OD) δ 23.9, 25.7, 27.3, 29.6, 31.6, 39.7, 40.6, 40.9, 42.1, 45.5, 60.5, 126.8, 126.9, 127.1, 128.4, 128.6, 129.2, 129.7, 130.3, 133.7, 134.7, 134.8, 158.5, 158.6, 162.7, 178.6; HRMS (FAB) *m/z* calcd for $C_{26}H_{38}N_7O$ (MH^+), 464.3138; found, 464.3147.

Density Functional Theory (DFT) Calculation. DFT calculations were carried out on a SGI Origin 3800 system within the Gaussian 98 package.[36] Geometry optimizations were performed by the B3LYP hybrid functional[37] with the basis set denoted as B3LYP/631A, which consists of the Ahlrichs all-electron SVP basis set[38] for Cu and 6-31G(d)[39] for the rest. The geometry of the transition state (**45**) was optimized by QST2 transition state search from the optimized structures **43** and **46**. The number of imaginary frequencies of these optimized structures was confirmed by frequency analysis (**43** and **46**, 0; **45**, 1).

[^{125}I]-SDF-1 Binding and Displacement. Stable CHO cell transfectants expressing CXCR4 variants were prepared as described previously.[40] CHO transfectants were harvested by treatment with trypsin-EDTA, allowed to recover in complete growth medium

(MEM-α, 100 μg/mL penicillin, 100 μg/mL streptomycin, 0.25 μg/mL amphotericin B, 10% (v/v)) for 4 to 5 h, and then washed in cold binding buffer (PBS containing 2 mg/mL BSA). For ligand binding, the cells were resuspended in binding buffer at 1×10^7 cells/mL, and 100 μL aliquots were incubated with 0.1 nM of [^{125}I]-SDF-1 (PerkinElmer Life Sciences) for 2 h on ice under constant agitation. Free and bound radioactivity were separated by centrifugation of the cells through an oil cushion, and bound radioactivity was measured with a gammma-counter (Cobra, Packard, Downers Grove, IL). Inhibitory activity of compound **62** was determined based on the inhibition of [^{125}I]-SDF-1-binding to CXCR4 transfectants (IC_{50}).

Acknowledgment. We thank Dr. Motoo Shiro, Rigaku International Corporation, Japan, and Dr. Terrence R. Burke, Jr., NCI, NIH, U.S.A., for X-ray analysis and for proofreading this manuscript, respectively. Computation time was provided by the Supercomputer Laboratory, Institute for Chemical Research, Kyoto University. This research was supported in part by 21st Century COE Program "Knowledge Information Infrastructure for Genome Science", a Grant-in-Aid for Scientific Research from the Ministry of Education, Culture, Sports, Science and Technology, Japan, Philip Morris U.S.A., Inc., Philip Morris International, and the Japan Health Science Foundation. A.N. and Y.S. are grateful for research fellowships of the JSPS for Young Scientists.

Supporting Information Available: Experimental details. Alternative synthetic route of S_N2-**25**. Determination of the relative configuration of **53** and **59**. ORTEP diagrams and CIF files for X-ray structures of **28** and **33**. Optimized coordinates and energies of complexes **43**, **45**, and **46**. ^{1}H and ^{13}C NMR spectra of representative compounds. This material is available free of charge via the Internet at http://pubs.acs.org.

JO060390T

(36) Frisch, M. J.; Trucks, G. W.; Schlegel, H. B.; Scuseria, G. E.; Robb, M. A.; Cheeseman, J. R.; Zakrzewski, V. G.; Montgomery, J. A., Jr.; Stratmann, R. E.; Burant, J. C.; Dapprich, S.; Millam, J. M.; Daniels, A. D.; Kudin, K. N.; Strain, M. C.; Farkas, O.; Tomasi, J.; Barone, V.; Cossi, M.; Cammi, R.; Mennucci, B.; Pomelli, C.; Adamo, C.; Clifford, S.; Ochterski, J.; Petersson, G. A.; Ayala, P. Y.; Cui, Q.; Morokuma, K.; Malick, D. K.; Rabuck, A. D.; Raghavachari, K.; Foresman, J. B.; Cioslowski, J.; Ortiz, J. V.; Stefanov, B. B.; Liu, G.; Liashenko, A.; Piskorz, P.; Komaromi, I.; Gomperts, R.; Martin, R. L.; Fox, D. J.; Keith, T.; Al-Laham, M. A.; Peng, C. Y.; Nanayakkara, A.; Gonzalez, C.; Challacombe, M.; Gill, P. M. W.; Johnson, B. G.; Chen, W.; Wong, M. W.; Andres, J. L.; Head-Gordon, M.; Replogle, E. S.; Pople, J. A. *Gaussian 98*, revision A.11; Gaussian, Inc.: Pittsburgh, PA, 1998.

(37) (a) Becke, A. D. *J. Chem. Phys.* **1993**, *98*, 5648. (b) Lee, C.; Yang, W.; Parr, R. G. *Phys. Rev. B: Condens. Matter* **1988**, *37*, 785.

(38) Schäfer, A.; Horn, H.; Ahlrichs, R. *J. Chem. Phys.* **1992**, *97*, 2571.

(39) Hehre, W. J.; Radom, L.; von Ragué Schleyer, P.; Pople, J. A. *Ab Initio Molecular Orbital Theory*; John Wiley: New York, 1986.

(40) Navenot, J. M.; Wang, Z. X.; Trent, J. O.; Murray, J. L.; Hu, Q. X.; DeLeeuw, L.; Moore, P. S.; Chang, Y.; Peiper, S. C. *J. Mol. Biol.* **2001**, *313*, 1181.

Involvement of the CXCL12/CXCR4 Pathway in the Recovery of Skin Following Burns

Shani Avniel[1,9], Zaretski Arik[2,9], Alex Maly[3], Assa Sagie[2], Hanna Ben Basst[4], Merav Darash Yahana[1], Ido D. Weiss[1], Boaz Pal[1], Ori Wald[1], Dean Ad-El[5], Nobutaka Fujii[6], Fernando Arenzana-Seisdedos[7], Steffen Jung[8], Eithan Galun[1], Eyal Gur[2] and Amnon Peled[1]

Burn wound healing is a complex process consisting of an inflammatory phase, the formation of granulation tissue, and remodeling. The role of the CXCL12/CXCR4 pathway in the recovery of skin following burns is unknown. We found that CXCL12 is similarly expressed in human, swine, and rat skin by pericyte and endothelial cells, fibrous sheet, fibroblasts, and axons. Following burns, the levels of CXCL12 were markedly increased in human burn blister fluids. One day after injury, there was a gradual increase in the expression of CXCL12 in the hair follicles and in blood vessel endothelium surrounding the burn. Three to 11 days following burns, an increased number of fibroblasts expressing CXCL12 were observed in the recovering dermis of rat, swine, and human skin. In contrast to CXCL12, CXCR4 expression was detected in proliferating epithelial cells as well as in eosinophils and mononuclear cells infiltrating the skin. *In vitro*, CXCL12 was expressed by primary human skin fibroblasts, but not by keratinocytes, and was stimulated by wounding a confluent cell layer of these fibroblasts. Blocking the CXCR4/CXCL12 axis resulted in the significant reduction in eosinophil accumulation in the dermis and improved epithelialization. Thus, blocking CXCR4/CXCL12 interaction may significantly improve skin recovery after burns.

Journal of Investigative Dermatology (2006) **126,** 468–476. doi:10.1038/sj.jid.5700069; published online 22 December 2005

INTRODUCTION

Skin integrity is of importance for the protection and separation of body tissues from the surrounding environment. The loss of skin due to burns or trauma exposes the body to severe stress, impairing or even eliminating the many vital functions this organ performs (Clark, 1988; Cotran *et al.*, 1999). Full-thickness skin tissue is comprised of keratinocytes lined on a basement membrane, produced by fibroblasts and keratinocytes. Deeper layers of the skin include, in addition to fibroblasts, fat cells and multiple subsets of immune cells such as dendritic cells, lymphocytes, and polymorphonuclear cells. The complex organization of normal skin is designed to support the numerous functions of this organ as both an immunologic and a physical barrier. Nevertheless, not much is known about the factors responsible for the complex architecture of this organ under physiologic and pathologic conditions.

Stromal-derived factor-1 (CXCL12) controls many aspects of stem cell function. CXCL12 has been identified as a powerful chemoattractant for immature hematopoietic stem cells (Aiuti *et al.*, 1997). Mice that lack either CXCL12 or its receptor CXCR4 exhibit many defects, including impaired hematopoiesis in the fetal bone marrow (Nagasawa *et al.*, 1996; Ma *et al.*, 1998; Zou *et al.*, 1998; McGrath *et al.*, 1999). Recently, it was shown that mobilization, homing, and engraftment of hematopoietic stem cells as well as the trafficking of neuronal and primordial germ cells are dependent on the expression of CXCL12 and CXCR4 (Peled *et al.*, 1999; Doitsidou *et al.*, 2002). Furthermore, it was also shown that the expression of CXCL12 is upregulated following irradiation and hypoxia and that CXCL12 can induce the recruitment of endothelial progenitor cells in a regeneration model for myocardial infarction (Ponomaryov *et al.*, 2000; Askari *et al.*, 2003; Ceradini *et al.*, 2004). The regulation of CXCL12 and its physiological role in peripheral tissue repair remain incompletely understood. A recent study showed that CXCL12 gene expression is regulated by the transcription factor hypoxia-inducible factor-1 in endothelial cells, resulting in the selective *in vivo* expression of CXCL12 in ischemic tissue in direct proportion to reduced oxygen tension (Hitchon *et al.*, 2002; Schioppa *et al.*, 2003).

[1]*Goldyne Savad Institute of Gene Therapy, Hadassah University Hospital, Jerusalem, Israel;* [2]*Department of Plastic and Reconstructive Surgery, The Tel-Aviv Sourasky Medical Center, Pethach Tikva, Israel;* [3]*Department of Pathology, Hadassah University Hospital, Jerusalem, Israel;* [4]*Laboratory of Experimental Surgery, Hadassah University Hospital, Jerusalem, Israel;* [5]*Department of Plastic and Reconstructive Surgery, Rabbin Medical Center, Pethach Tikva, Israel;* [6]*Graduate School of Pharmaceutical Sciences, Kyoto University, Sakyo-ku, Kyoto, Japan;* [7]*Institute Pasteur, Paris, France and* [8]*Department of Immunology, Weizmann Institute of Science, Rehovot, Israel*

[9]*These authors contributed equally to this work.*

Correspondence: Dr Amnon Peled, Gene Therapy Institute, Hadassah University Hospital, PO Box 12000, Jerusalem, Israel. E-mail: peled@hadassah.org.il or Dr Eyal Gur, Department of Plastic and Reconstructive Surgery, Sourasky Medical Center, PO Box 64239, Tel-Aviv, Israel. E-mail: eyalgur@netvision.net.il

Abbreviations: mAB, monoclonal antibody; GFP, green fluorescent protein

Received 24 March 2005; revised 31 August 2005; accepted 7 September 2005; published online 22 December 2005

© 2005 The Society for Investigative Dermatology

Hypoxia-inducible factor-1-induced CXCL12 expression was suggested to increase the adhesion, migration, and homing of circulating CXCR4-positive progenitor cells to ischemic tissue.

Thus, CXCL12 plays an important role in the organization of tissues during development and following damage. CXCL12 is expressed by dendritic cells, fibroblasts, and endothelial cells in human skin (Pablos *et al.*, 1999). Here, we show that following burns, the levels of CXCL12 is markedly increased first in the burn blister and then in the junction tissues surrounding the burn, hair follicles, endothelium blood vessels and fibroblasts in the recovering dermis. Treatment of partial thickness burns in a rat model with antibodies to CXCR4 or the small peptide CXCR4 antagonist, 4F-benzoyl-TN14003 (Tamamura *et al.*, 2003), resulted in improved epithelialization and reduced eosinophilia. These observations suggest a role for eosinophils and the CXCL12/CXCR4 pathway in wound healing and in the recovery of burn skin.

RESULTS

CXCL12 is similarly expressed in human, swine, and rat normal skin

The expression of CXCL12 in normal skin was examined by immunohistochemical staining using monoclonal antibody (mAB) (MAB 350) (R&D Systems Inc., Minneapolis, Minnesota) against the chemokine CXCL12. We first examined the antibody crossreactivity of CXCL12 staining on liver sections of mouse, human, and rat, since previous studies have shown that CXCL12 is specifically expressed in the bile ducts and blood vessels of human liver (Wald *et al.*, 2004). In mouse, human, and rat, liver bile ducts were specifically stained with MAB 350 for CXCL12 (data not shown). Control stain without the primary Ab showed no staining. Using the same mAB staining for CXCL12 in human, swine, and rat, normal skin showed similar expression patterns. CXCL12 in human normal skin (Figure 1) was detected in the basal layer of the epidermis (Figure 1a), on scattered cells in the papillary dermis (Figure 1b), in pericytes, and in the endothelial layer of blood vessels (Figure 1c). The fibrous sheet of hair follicles (Figure 1d), sweat glands (not uniformly) (Figure 1e), axons, and small blood vessels in the nerve tissue (Figure 1f) also expressed CXCL12. No staining was detected with a control antibody used to stain identical skin sections (Figure 1g–h). CXCL12 was detected in rat normal skin on the basal layer of the epidermis (Figure 2a), on scattered cells in the papillary dermis (Figure 2b), and on pericytes and the endothelial layer of blood vessels (Figure 2c). The chemokine CXCL12 was also expressed by axons and small blood vessels in the nerve tissue (Figure 2d) and by fibrous sheet of hair follicles (Figure 2e). No staining was detected with control antibody used to stain the same skin sections (Figure 2f). The

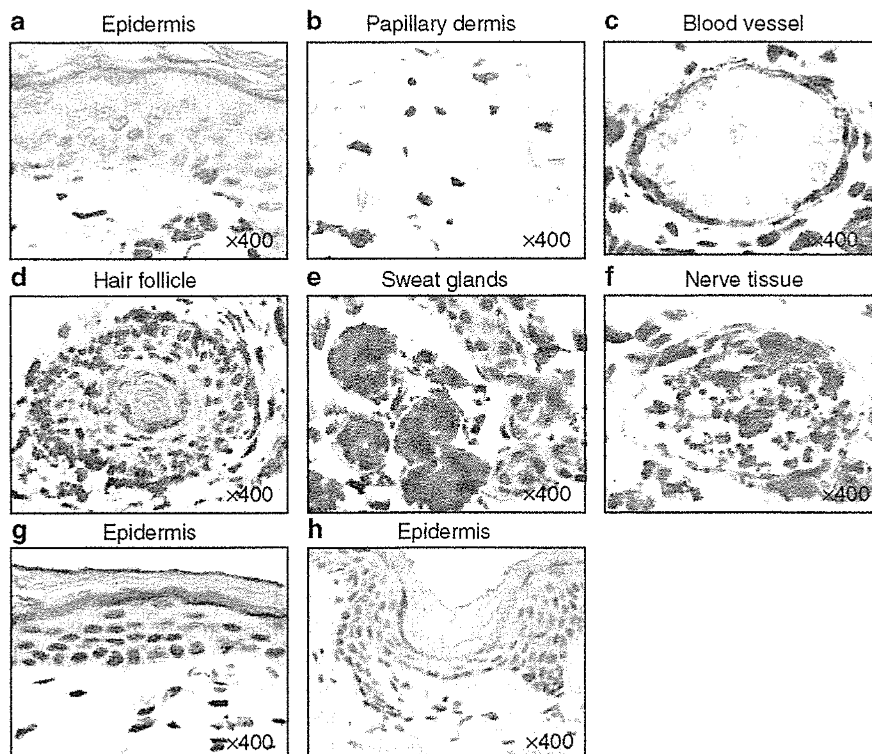

Figure 1. Expression of CXCL12 in normal human skin. Immunohistochemistry staining results using a monoclonal antibody against the chemokine CXCL12 on human normal skin section. **(a)** Stained cells in the basal layer of the epidermis. **(b)** Scattered cells stained in the papillary dermis. **(c)** Endothelial cells and pericytes stained in blood vessel. **(d)** Fibrous sheet stained in the hair follicle. **(e)** Sweat glands not uniformly stained. **(f)** Axons and blood vessels stained in nerve tissue. **(g)** Sections of epidermis and papillary dermis were stained without the primary antibody ensuring that no background staining was received from the second antibody. **(h)** Sections of epidermis and papillary dermis were stained with the primary antibody after incubation with CXCR4 ligands CXCL12α and CXCL12β ensuring that the staining is specific for CXCL12. (Original magnification × 400).

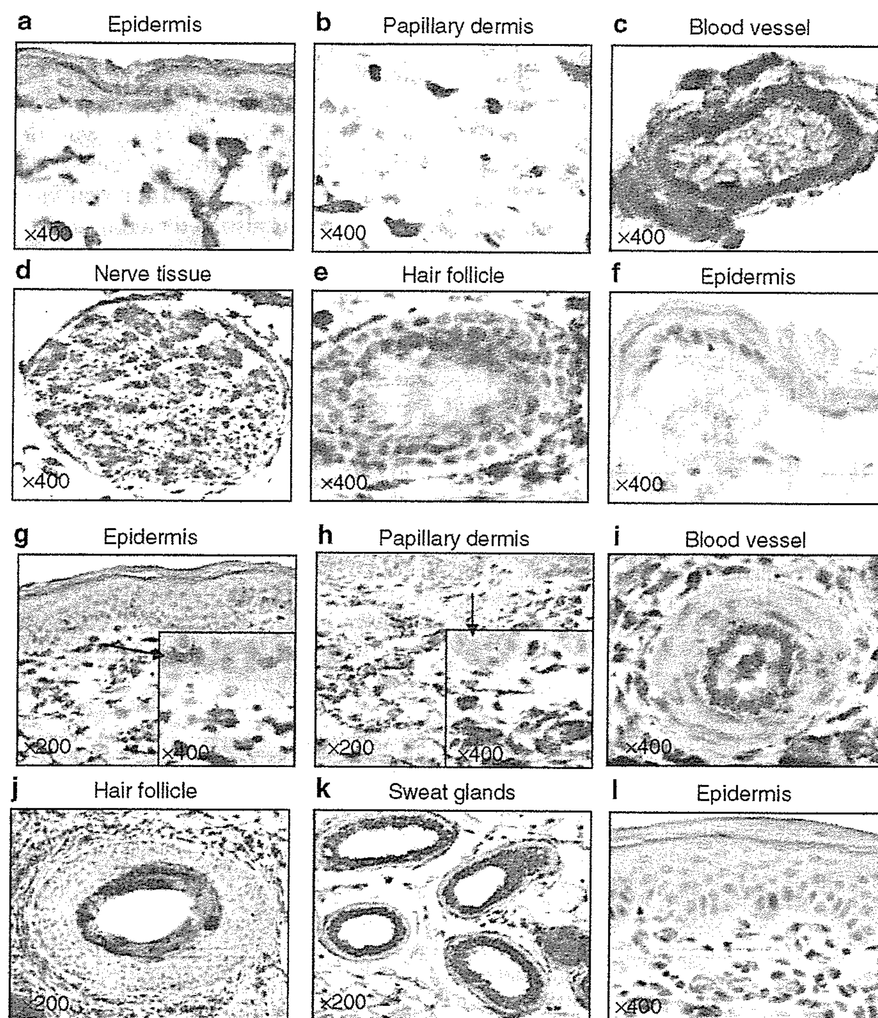

Figure 2. Expression of CXCL12 in rat and swine normal skin. (a–f) Immunohistochemical staining results using monoclonal antibody against the chemokine CXCL12 on rat normal skin sections. (a) Cells stained in the basal layer of the epidermis. (b) Scattered cells stained in the papillary dermis. (c) Endothelial cells and pericytes stained in blood vessel. (d) Axons and blood vessels stained in nerve tissue. (e) Fibrous sheet stained in the hair follicle. (f) Epidermis and papillary dermis control staining, without the primary antibody (original magnification of × 400). (g–l) Immunohistochemical staining results using monoclonal antibody against the chemokine CXCL12 on swine normal skin sections. (g) Cells stained in the basal layer of the epidermis and the papillary dermis. (h) Scattered cells stained in the papillary dermis. (i) Endothelial cells and pericytes stained in blood vessel. (j) Fibrous sheet stained in the hair follicle. (k) Sweat glands staining. (l) control staining, without the primary antibody. (Original magnifications × 200 or × 400).

chemokine CXCL12 was similarly expressed by swine normal skin cells in the basal layer of the epidermis (Figure 2g), by scattered cells in the papillary dermis (Figure 2h), in pericytes, and by the endothelial layer of blood vessels (Figure 2i). The chemokine CXCL12 was also expressed by fibrous sheets of hair follicles (Figure 2j) and by sweat glands (Figure 2k). No staining was detected with control antibody used to stain the same skin sections (Figure 2l). This unique and conserved expression pattern of CXCL12 may suggest a role for CXCR4/CXCL12 axis in the organization of skin tissue.

Following burns, the level of CXCL12 was markedly increased in human burn blister fluids, hair follicles, blood vessels endothelium, and fibroblasts in the recovering dermis of rat, swine, and human skin.

In order to study the effect of burn injury on CXCL12 expression in the skin, we first collected burn wound fluids, and CXCL12 levels were measured by ELISA assay and compared to the levels of IL-8 (Figure 3a and b). The results indicate a unique pattern of the chemokine CXCL12 expression compared to the IL-8. IL-8 appeared first in the burn fluid a few hours after injury, reached a plateau level after 1 day, and remained at the same level for the next 4 days. CXCL12 appeared a few hours after injury, reached a plateau level after 1 day, and remained at the same level for an additional 2 days, and then the level of CXCL12 decreased exponentially. The consistent overexpression of IL-8 in burn wound fluids and skin tissue has also been reported by others (Iocono *et al.*, 2000). These authors suggested that IL-8 has a role in stimulating neutrophils

migration and accelerating the angiogenic process within the burn wound.

The expression of the chemokine CXCL12 following burn infliction was further examined by immunohistochemical staining of rat skin sections. The results shown in Figure 5 indicate accumulation of CXCL12 in the rat burned skin in correlation with time. Six days and 1 day after injury, CXCL12 was not detected in the burned tissue. Three days postburn, CXCL12 was detected in endothelium blood vessels, in the hair follicles, and also in scattered cells accumulated in the dermis. Five and 7 days postburn, a higher expression of the chemokine was detected in blood vessels and in fibroblast-like cells accumulated in the dermis. As was shown before for human normal skin, CXCR4 was detected in normal and proliferating rat epithelial cells and endothelial cells after burn injury (Figure 4). In the dermis of injured skin, CXCR4 expression was also detected in mononuclear cells as well as infiltrating eosinophils.

The pattern of CXCL12 expression in swine skin postburn is similar. Four days postburn, CXCL12 was present in endothelium blood vessels and in scattered cells that accumulated in the papillary dermis. Ten days after injury, a strong expression of the chemokine was detected in blood vessels and in the accumulating fibroblast-like cell population in the papillary dermis of normal skin stained for CXCL12 is shown in Figure 5c.

In order to determine the cell types that expressed high levels of CXCL12, we stained parallel sections from burned skin for vimentin and CXCL12. The majority of fibroblast-like cells were stained for both CXCL12 and vimentin indicating that fibroblasts were expressing CXCL12 in the skin following

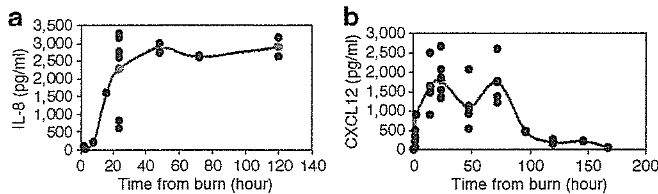

Figure 3. (a) IL-8 and (b) CXCL12 mean levels (pg/ml) in human burn wound fluid collected from blisters of patients with second degree burn. Fluids were collected 0–5 days after burn as a medical treatment protocol. Samples were measured for the chemokines by ELISA assays. Each point represents one patient.

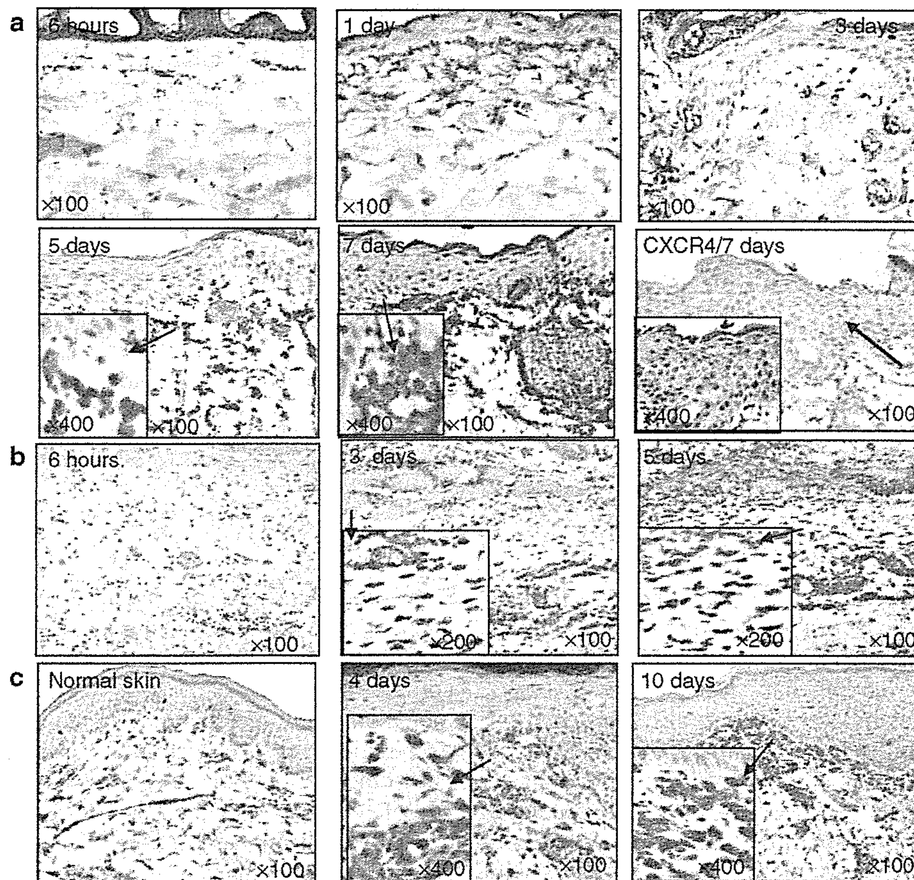

Figure 4. The involvement of CXCL12 in rat and swine burn wound healing. Expression of CXCL12 in rat burn wound healing. (**a**) Immunohistochemical staining of CXCL12 of rat epidermis burned skin sections, at 6 hours, 1 day, 3 days, 5 days, and 7 days after the burn. Staining for CXCR4 is shown at 7 days after the burn (original magnifications × 100, × 200). (**b**) Immunohistochemical staining of CXCL12 of rat dermis burned skin sections, at 6, 72, and 120 hours after the burn (original magnifications × 100, × 200). (**c**) Expression of CXCL12 in swine skin after second-degree burn. Immunohistochemical staining of CXCL12 at 4 days, 10 days after the burn, and at time 0 in normal skin. (Original magnifications × 100, × 400).

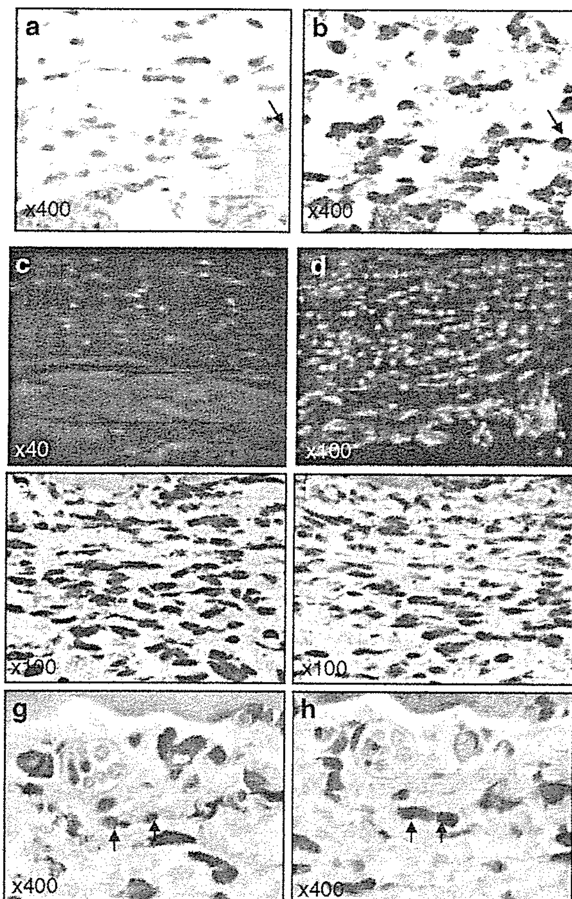

Figure 5. Coexpression of vimentin and CXCL12 in rat burned skin. (**a**) Immunohistochemical staining for vimentin of rat burned skin dermis 5 days after burn. (**b**) CXCL12 immunohistochemical staining of consecutive tissue section of rat burned skin section 5 days after burn (Original magnification ×400; arrow indicates the staining for CXCL12 and vimentin). Coexpression of GPF and CXCL12 in heterozygous mice bearing a GFP reporter knocked-in to the CX3CR1 locus burned skin. (**c** and **d**) Accumulation of GFP+ monocyte/dendritic cells in the dermis of injured skin. (**e–h**) Coexpression of GFP+ CXCL12 in monocyte/dendritic cells in parallel sections from dermis of injured skin; arrow indicates the staining for CXCL12 and GFP.

burn injury (Figure 5a and b). However, part of the cells that expressed CXCL12 did not express vimentin. CXCL12 was shown to be expressed by human dendritic cells localized to the epidermis and the dermis (Pablos *et al.*, 1999). An excellent means to track monocyte subsets in the skin was through the use of mice bearing a green fluorescent protein (GFP) reporter knocked-in to the CX3CR1 chemokine receptor locus (Qu *et al.*, 2004). Indeed, we found that following injury, monocyte with a dendritic-like shape accumulated in the dermis and epidermis (Figure 5c and d). Part of the monocyte/dendritic cells that expressed the GFP also expressed CXCL12 (Figure 5e–h).

To further study the expression of CXCL12 and CXCR4 in the skin, we used primary skin fibroblast and keratinocyte cultures. In agreement with our *in vivo* results, we found that while the fibroblasts expressed the chemokine CXCL12 in the mRNA level, the keratinocytes did not. In contrast to CXCL12, keratinocytes, but not the fibroblasts, expressed the receptor CXCR4. In order to verify our finding, we used ELISA assay to check the production of CXCL12 by keratinocytes and fibroblasts. The results demonstrated that while keratinocytes did not express the chemokine CXCL12 at the protein level, fibroblasts did express and secrete CXCL12 (Figure 6a), especially during the recovery of skin fibroblasts migrating into the wound area and accumulating in the dermis. In order to study the effect of wounding on CXCL12 expression by skin fibroblasts, a "scratching" assay was performed on confluent layers of human skin fibroblasts *in vitro*. Immunohistochemical staining of confluent human skin fibroblasts showed moderate CXCL12 expression. Two days following scratching, an increase in CXCL12 expression by cells adjacent to the affected area was detected (Figure 6d). Fibroblast monolayers were negatively stained with control antibody against cytokeratin.

Inhibition of the CXCL12/CXCR4 pathway resulted in reduced eosinophil accumulation and improved epithelialization

In order to evaluate the effect of the CXCR4 antagonist, 4F-benzoyl-TN14003, and neutralizing antibodies to the receptor on the recovery of rat skin, we first tested their ability to inhibit the migration of rat lymphocytes in response to CXCL12. Migration assay was carried out on total rat lymphocytes separated by Ficoll gradient, and their migrating ability to medium containing CXCL12 was examined. Lymphocytes were incubated with the CXCR4 antagonist, 4F-benzoyl-TN14003, and an antibody against CXCR4. Treatment of cells with 4F-benzoyl-TN14003 exerted a strong inhibitory effect, whereas treatment of cells with neutralizing antibodies to CXCR4 exerted moderate effect on the migration of cells in response to CXCL12 (Figure 7a).

Next, we examined the inhibitory effect of CXCR4 antagonists on burn wound healing (Figure 7b–d). Inhibitors were injected subcutaneously to the burned area at 0, 1 day, and 3 days, and animals were killed 5 days postburn. Animals injected with the CXCR4 inhibitor, 4F-benzoyl-TN14003, showed an increased epithelialization (Figure 7b). A small but not significant decrease in the polymorphonuclear cell population in the dermis was observed (Figure 7c). However, a strong and significant inhibition in eosinophil accumulation in the dermis was found in the 4F-benzoyl-TN14003 and antibodies to the CXCR4-treated groups (Figure 7d). In contrast to eosinophil accumulation, the accumulation of polymorphonuclear cell population in the epidermis was not affected (Figure 7d). These results suggest a role for CXCR4/CXCL12 interaction in the migration of eosinophils to the skin in the process of epithelialization following burn inflection.

DISCUSSION

Burn wound healing is a complex process consisting of an early phase of energy depletion and necrosis, followed by a two-stage inflammatory phase, formation of granulation tissue, matrix formation, and remodeling (Clark, 1988; Cotran et al., 1999; Spies *et al.*, 2002). The numerous cellular and humoral interactions during these phases of thermal wound healing are complex and not well understood. Partial skin

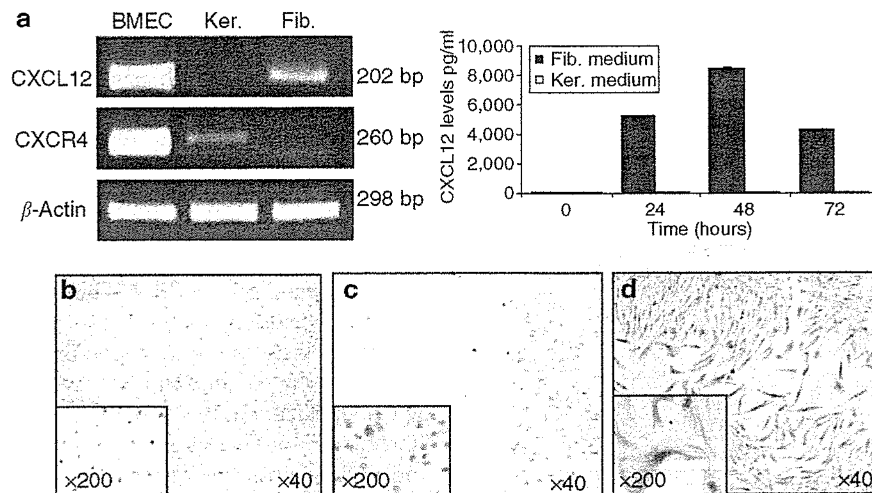

Figure 6. CXCL12 is expressed in primary cultures of fibroblasts, but not in keratinocytes. (**a**) *In vitro* expression of CXCL12 and CXCR4 in keratinocytes and fibroblasts. Expression of CXCL12 and CXCR4 measured by RT-PCR in primary human keratinocytes and fibroblasts. Expression of CXCL12 in keratinocytes- and fibroblasts-conditioned medium as measured by ELISA assay. (**b**) Immunostaining of human primary fibroblasts with anti-cytokeratin antibodies as control. (**c**) Immunostaining of human primary fibroblasts with anti CXCL12 antibodies. (**d**) Immunostaining of human primary fibroblasts with anti-CXCL12 of human primary fibroblast 2 days after wounding the fibroblasts monolayer. (Original magnifications × 40 and × 200). Fib.=fibroblasts; Ker.=keratin.

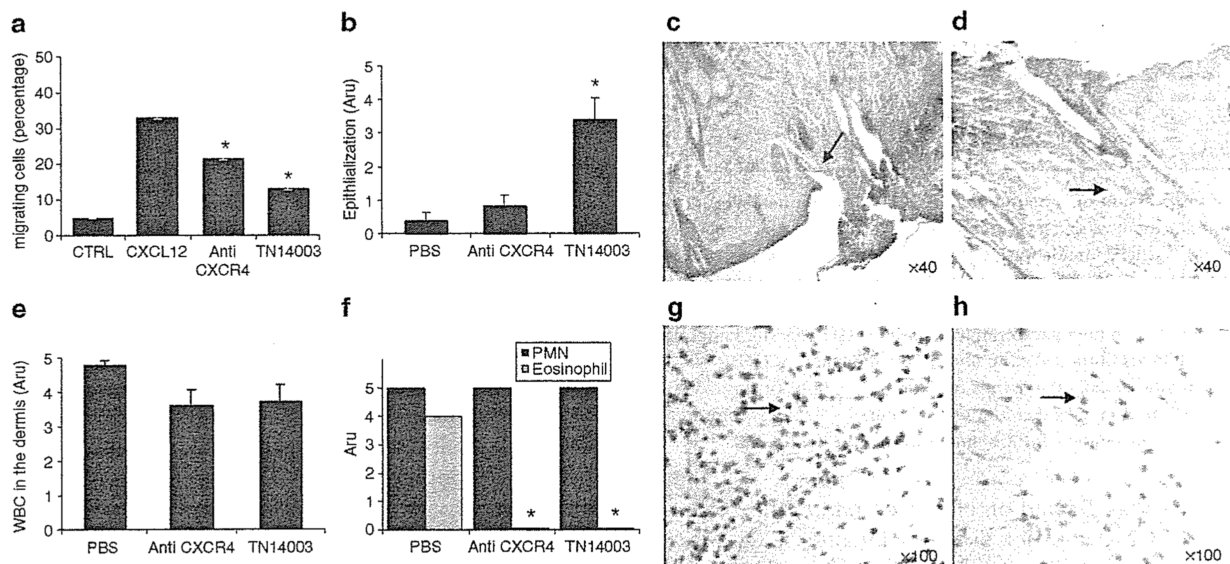

Figure 7. Effect of neutralizing antibodies to CXCR4 and the small peptide inhibitor of CXCR4 on inflammation and regeneration of skin following burns. (**a**) Migration of rat lymphocytes in response to CXCL12 (100 ng/ml) was tested in the absence and presence of neutralizing antibodies to CXCR4 (NA), or the CXCR4 antagonist – 4F-benzoyl-TN14003. (**b**) The effect of CXCR4 antagonists on re-epithelialization. (**c**) Depicts the epithelialization of burned skin in mice treated with phosphate-buffered saline (PBS) (asterisk indicates the sites of novel epithelialization). (**d**) Depicts the epithelialization of burned skin in mice treated with 4F-benzoyl-TN14003 (asterisk indicates the sites of novel epithelialization). The number of lymphocytes in the dermis is shown in (**e**). The number of polymorponuclear cells (PMN) in the epidermis and eosinophils in the dermis 5 days after burn is shown in (**f**). (**g**) Depicts the eosinophils in the dermis of mice treated with PBS (arrow indicates the site of eosinophilia). (**h**) Depicts the eosinophils in the dermis of mice treated with 4F-benzoyl-TN14003 (arrow indicates the site of eosinophilia). The results are the average of two experiments; for each experiment at least five rats were tested ($P<0.05$).

burn wounds could be more effectively treated sooner if the blister wall was maintained intact (Ono *et al.*, 1995). Burn wound fluids from blisters contain relatively large amounts of cytokines such as platelet-derived growth factor, IL-6, transforming growth factor-β, and IL-8 thought to stimulate the wound healing process by regulating epithelialization (Ono *et al.*, 1995; Struzyna *et al.*, 1995). The increased CXCL12 levels in human burn fluid during the first 3 days following burn injury (Figure 3b) and the expression of CXCR4 by human keratinocytes (Figure 4a) may support the survival and tissue organization of these cells. This concept is supported by studies showing that CXCR4 is expressed by

skin keratinocytes and is essential for keratinocytes that participate in maintaining skin integrity (Smith *et al.*, 2004). The restricted presence of functional CXCL12 (24–48 hours following burn) may suggest a protective role for CXCL12 in the maintenance of skin tissue following burn. In contrast to the presence of CXCL12 in human burn fluid during the first 3 days following injury, an increased number of fibroblasts and dendritic cells that expressed CXCL12 are observed in the regenerating skin in the first 2 weeks following damage. This difference may be the result of increased levels of proteolytic activity in the burn fluid. Indeed, a variety of proteolytic enzymes such as cathepsin G, elastase, and matric metalloproteinase-9 were recently shown to degrade CXCL12 (Petit *et al.*, 2002).

In partial-thickness burns, the epidermis and the superficial dermis are destroyed and undergo necrosis (Clark, 1988; Cotran *et al.*, 1999; Singer and Clark, 1999). Twenty-four hours to 2 days following burns, the affected area lost CXCL12 expression. However, the expression of CXCL12 in the area adjacent to the burn wound was intensed. During this time period, a massive influx of neutrophils into the wound area was observed. The accumulation of neutrophils could not be blocked by CXCR4 antagonists, suggesting that CXCR4/CXCL12 axes have no detectable role in this process. The accumulation of neutrophils in the wound area was associated with an increased production of the neutrophil chemoattractants neutrophil activating protein-2 (NAP-2), Growth-Regulated Oncogene alpha (GRO-α), and Epithelial neutrophil activating peptide-78 (ENA-78), as well as with the sustained production of IL-8 in human burn blisters in human (Figure 3a) (Faunce *et al.*, 1999; Piccolo *et al.*, 1999; Gillitzer and Goebeler, 2001). In partial-thickness burns, the proliferating and migrating epithelium arose from the wound border as well as from hair follicles. The rate of epithelial cover was modulated by growth factors that stimulated the proliferation and chemotaxsis of epithelial cells (Clark, 1988; Cotran *et al.*, 1999; Singer and Clark, 1999). During the granulation phase, beginning 2–3 days following damage, fibroblasts attracted by macrophages migrated into the wound area; these fibroblasts from swine and rat origin secreted high levels of CXCL12 (Figures 4 and 5). The process of granulation is associated with intense angiogenesis (Cotran *et al.*, 1999; Singer and Clark, 1999). In parallel to migration of fibroblasts expressing high levels of CXCL12, novel and resident endothelial cells lining the blood vessels also expressed CXCL12. During this phase of wound healing, a second wave of immune cells entered the epidermis underlying the burn. These cells include macrophages, lymphocytes, and eosinophils. The chemokines CCL2, CXCL10, CXCL9, and CCL22 were found to be spatially associated with lymphocyte and monocyte accumulation (Gibran *et al.*, 1997; Gillitzer and Goebeler, 2001). We found a minor effect of CXCR4 antagonists on the recruitment of macrophages and lymphocytes, whereas the recruitment of eosinophils was totally blocked (Figure 7).

A fine balance between fibrotic tissue deposition and neovascularization on the one hand and fibrotic tissue degradation and epithelization on the other should be maintained in order to assure successful wound healing. Immune cell subpopulation recruited to the burned site is involved in orchestrating these events. Unbalanced proliferation and activation of fibroblasts may lead to inadequate granulation and the formation of a fibrotic tissue. However, reduced angiogenesis and blood flow into the burn wound can prevent successful epithelialization and wound repair. With regard to the CXCL12/CXCR4 axis, we have found that the most dramatic effect of CXCR4 antagonists was on the number of infiltrating eosinophils. The decrease in eosinophil migration into the wounded tissue and the increased epithelialization observed in mice treated with CXCR4 antagonist indicate that CXCL12/CXCR4 interactions are involved in shaping the balance between fibrosis and epithelialization. Moreover, these data may suggest that eosinophils are linked to the regulation of epithelialization.

Indeed, it was reported by Yang *et al.* (1997) that anti-interleukin-5 mAB (TRFK-5) treatment can deplete eosinophils in healing of cutaneous wounds and that wound closure by re-epithelialization in the treated animals was 4 days faster than in the control group. This study suggests a role for eosinophils in negatively affecting wound re-epithelialization. Neutralizing antibodies to CXCR4 and AMD3100, an antagonist of CXCR4/CXCL12 interaction, were shown to reduce lung eosinophilia, indicating that CXCR4-mediated signals contribute to lung inflammation in a mouse model of allergic airway disease (Gonzalo *et al.*, 2000; Lukacs *et al.*, 2002). Eosinophils constitutively express CC chemokine receptor 3 and, to a lesser extent, CC chemokine receptor 1. CC chemokine receptor 3 is mainly responsible for migration of resting eosinophils, and its specific ligand, eotaxin, represents the most potent chemoattractant for eosinophils (Nagase *et al.*, 2001b). However, eosinophils in inflamed tissue sites exhibited a decreased CC chemokine receptor 3 and an increased CXCR4 expression (Nagase *et al.*, 2001a). Surface CXCR4 protein was hardly detectable in the peripheral blood or freshly isolated eosinophils. Similarly to the phenomenon observed with eosinophils in inflamed tissues, surface expression of CXCR4 became gradually apparent during *in vitro* incubation of cells. CXCL12, the natural ligand of CXCR4, elicited an apparent Ca^{2+} influx in these cells and induced a strong migratory response comparable to that by eotaxin (Nagase *et al.*, 2000)

In summary, we suggest that the presence of CXCL12 in burn blisters is involved in protecting the skin during a short period of time following skin burn injury. Thereafter, CXCL12 expressed by fibroblasts and endothelial cells may induce the accumulation of eosinophils, which in turn slow the epithelialization. Our data suggest that CXCL12 is more predominantly supporting fibrosis than epithelialization. Indeed, we and others have recently shown that during liver fibrosis, the levels of CXCL12 expression by endothelial cells and fibroblasts are dramatically increased (Wald *et al.*, 2004). It is therefore possible that by using inhibitors against CXCR4, the balance between fibrosis and epithelialization can be changed, thereby leading to a better and faster recovery of skin following damage.

MATERIALS AND METHODS

Human cell lines

Human skin fibroblasts and keratinocytes were obtained from skin biopsies. Fibroblasts were grown in Dulbecco's modified Eagle's medium (DMEM) containing 10% fetal calf serum, and keratinocytes were cultured in H. Green keratinocyte-specific medium (Green *et al.*, 1979). Keratinocytes and fibroblasts were kindly provided by Professor Ben-Basst Laboratory, Hadassah University Hospital, Jerusalem, Israel. Cells were passaged weekly by trypsinization. Bone marrow endothelial cells are microvascular endothelial cells isolated from human bone marrow aspirates. The bone marrow endothelial cell-1 cell line was kindly provided by S Rafii. This cell line was generated by introducing the SV40-large T antigen into an early passage of primary bone marrow endothelial cell, and it has retained the morphology, phenotype, and function of the primary bone marrow endothelial cell. The bone marrow endothelial cell-1 cells were cultured in a complete DMEM and were passaged weekly by trypsinization.

Immunohistochemistry and *in vitro* scratched assay

Skin tissue samples were routinely fixed with formalin and embedded in paraffin. Antigen retrieval was performed in ethylenediaminetetraacetic acid buffer for 15 minutes in microwave, and sections were stained with mAB (MAB 350) (R&D Systems Inc., Minneapolis, MN) for CXCL12 (1:100) mAB′ against cytokeratins 1, 5, 15, and 10 (M0630) (DAKO, Glostrup, Denmark) and mAB anti-vimentin (M7020) (DAKO), mAB against rat CXCR4 (Torrey Pines Biolabs, Houston, TX), using biotinylated secondary polymer (87–9,963) (Zymed) based on standard indirect avidin–biotin horseradish peroxidase method, according to the manufacturer's instructions. 3-amino-9-ethylcarbazole was used for color development and sections were counterstained with hematoxylin. Cell immunohistochemistry staining: keratinocyte and fibroblast monolayers were grown in a tissue culture 6 mm plates. Then, cells were scratched using a 200 μl pipette, washed three times with phosphate - buffered saline (PBS), and grown in DMEM with 1% fetal calf serum. After 2 days, cells were fixed using 4% paraformaldehyde and stained for the chemokine CXCL12 as described previously.

ELISA assay and RT-PCR

ELISA assays for CXCL12 and IL-8 in burn fluids of fibroblast and keratinocyte medium were performed using the Quantikine kit (R&D Systems Inc., Minneapolis, Minnesota), according to the manufacturer's instructions. The expression levels of the chemokine CXCL12 and the chemokine receptor CXCR4 were determined by RT-PCR analysis. Total RNA was isolated from primary fibroblast and keratinocyte cultures. Each RNA sample was subjected to cDNA synthesis, and then semiquantative PCR was performed with specific primers at appropriate annealing temperatures. The resulting PCR products were separated on 1% agarose gel.

Transwell migration assays

Rat peripheral blood cells were loaded on Ficoll (Histopaque-1077-1, Sigma), and the peripheral blood mononuclear cells were isolated. Rat peripheral blood mononuclear cell migration was assessed in 24-well chemotaxis chambers (6.5-mm diameter, 5-mm pore polycarbonate transwell culture insert; Costar, Cambridge, Massachusetts). RPMI 1640 (600 μl) with 1% BSA (migration buffer) with or without 100 ng/ml of CXCL12α (Peprotech, Rehovot, Israel) were added to the lower wells, and 2×10^5 cells suspended in 100 μl of RPMI 1640 with 1% BSA were added to the upper wells. After 3 hours incubation, the membrane was removed and migrating cells were counted for 1 minute using fluorescence activated cell sorter.

Tissue collection, histological evaluation of the burn lesion

Human skin tissue samples were obtained from the Plastic Surgery Department, Souraski Medical Center, Tel-Aviv. In order to examine the different phases in burn wound healing and the involvement of the chemokine CXCL12 and the receptor CXCR4, the following experiments were carried out. Wistar female rats were anesthetized and their back was shaved. Burns (1 cm^2) were inflicted with a metal rod that has been immersed in a hot boiling water bath and laid on the posterior part of the hip and back for 2–3 seconds. All experiments were approved by the Animal care committee of the Medical Center, Tel-Aviv and the Hebrew University. All the material collected from human specimens was approved by Tel-Aviv Sourasky Medical Center Institutional Committee and in adherence to the Declaration of Helsinki Principles. Heterozygous mice bearing a GFP reporter knocked-in allele to the CX3CR1 locus (Qu *et al.*, 2004) were maintained at the Weizmann Institute of Science Animal Facility. Each group of three rats was injected subcutaneously with either PBS, anti-CXCR4, or with 4F-benzoyl-TN14003 to the burned area. Animals were killed at the indicated times after burn infliction: 0, 6 hours, 1 day, 3 days, 5 days, and 7 days. Histopathological diagnosis was confirmed for each specimen. Histological sections were prepared from formalin-fixed, paraffin-embedded tissues stained with hematoxylin and eosin. The evaluation to the level of epithelialization and white blood cells in the epidermis and dermis was made to each section by a scale from 1 to 5. The sections were scored by two independent pathologists. Treated rats were injected subcutaneously to the burned area with one of the following: PBS, mAB against rat CXCR4, the small peptide CXCR4 inhibitor, or 4F-benzoyl-TN14003. All animals were killed 120 hours after injury. Histopathological diagnosis was confirmed for each specimen. Histological sections were prepared from formalin-fixed, paraffin-embedded tissues stained with hematoxylin and eosin. The evaluation to the level of epithelialization and white blood cells in the dermis was made to each section by a scale from 1 to 5. The grading scale was as follows: 0 = no inflammation or epithelialization; 1 = low inflammation or epithelialization; 2 = low to moderate inflammation or epithelialization; 3 = moderate inflammation or epithelialization; 4 = high inflammation or epithelialization; and 5 = very high inflammation or epithelialization.

Swine burned skin paraffin-embedded sections were provided by the Laboratory of Experimental Surgery, Hadassah University Hospital, Jerusalem, Israel. All experiments were approved by the Animal Care Committee of the Hebrew University. Burn blister fluid collection was collected at the Plastic Surgery Department, Souraski Medical Center, Tel-Aviv, Israel as a medical procedure. The blister fluid was examined for the chemokine CXCL12 levels by ELISA assay, and for the levels of IL-8.

Statistical analysis

Results are expressed as mean $\pm$ SD. Statistical differences were determined by an analysis of two-tailed Student's *t*-test.